

Manuscript Number: ATE-2015-9618

Title: Simulation of engagement control in automotive dry-clutch and temperature field analysis through finite element model

Article Type: Research Paper

Keywords: dry-clutch; friction coefficient; temperature; finite element analysis; engagement driving

Corresponding Author: Dr. Mario Pisaturo, Ph.D.

Corresponding Author's Institution: University of Salerno

First Author: Mario Pisaturo, Ph.D.

Order of Authors: Mario Pisaturo, Ph.D.; Adolfo Senatore, prof.

Abstract: The tribological contact under sliding condition in the clutch facing surfaces during the engagement manoeuvre is strongly affected by heat transfer occurring in the system. The frictional forces acting on the contact surfaces produce mechanical energy losses which are converted in heat with ensuing temperature increase.

Reports about the temperature rise after repeated clutch engagements prove the occurrence of interface temperature peaks as high as 300°C.

Unfortunately, only few papers address their focus toward experiments and their outcomes about the influence of temperature and the other operating parameters on the frictional behaviour of the clutch facing materials.

In this paper, the Authors mainly explored the frictional behaviour modification for thermal level higher than 250-300°C, whose effect is a sharp decline of the friction coefficient related to the decomposition of the phenol resin of the facings. Moreover, this phenomenon induces not expected transition from dry friction to mixed dry-lubricated friction which explains the reasons of the friction coefficient drop. The temperature affects also the cushion spring load-deflection characteristic and the ensuing transmitted clutch torque.

Thus, an original frictional map has been implemented in a control algorithm to estimate the heat flux during vehicle launch and up-shift manoeuvres. The results of the longitudinal vehicle dynamics has been used in a FEA to predict the temperature field during repeated clutch engagement on the contact surfaces. The simulation results prove that during each engagement the interface temperature increases of 30-35°C. This means that after only few repeated clutch engagements the temperature field could reach values near the critical point of 300°C.

In such a way, this paper aims at providing useful references to control engineers in order to improve the dry-clutch transmissions performances.

Cover letter

Dear Editor,

as Authors of the paper “Simulation of engagement control in automotive dry-clutch and temperature field analysis through finite element model” submitted to this prestigious journal, we would like to briefly describe its main objectives.

Our research work could be classified in the area of automotive system and in particular it deals with the study of accurately estimate the temperature field in a dry-clutch during the engagement manoeuvres, start-up and gear-shift. To this aim, typical manoeuvres have been evaluated and implemented in a suitable control strategy based on the multiple Model Predictive Control (mMPC) designed to track reference trajectories both for the engine and clutch angular speed. Moreover, the controller takes into account the actuator and engine dynamics and a detailed dry-clutch behaviour. Thus, an original frictional map has been implemented in a control algorithm to estimate the heat flux during vehicle launch and up-shift manoeuvres. The results of the longitudinal vehicle dynamics has been used in a FEA to predict the temperature field during repeated clutch engagement on the contact surfaces. In the proposed FE model the clutch facing material and the pressure plate have been modelled to get the temperature distribution due to the frictional energy. The simulation results prove that after repeated clutch engagements the temperature field reaches values near the critical point of 300°C.

The outcome of this analysis could become a key element for designers of automated clutches and control engineers to improve the dry-clutch transmissions performances.

Of course, we will be pleased to read the reviewers’ comments in order to improve the paper quality and better fit the journal purpose.

Best Regards,
The Authors.

Suggested Reviewers

A. A. Yevtushenko, a.yevtushenko@pb.edu.pl, Faculty of Mechanical Engineering, Bialystok University of Technology

Michael Mitariu, mitariu@ipek.uni-karlsruhe.de, Institute of Product Development (IPEK), University of Karlsruhe (TH) Research University

Oday I. Abdullah, oday.abdullah@tu-harburg.de, System Technology and Mechanical Design Methodology, Hamburg University of Technology

HIGHLIGHTS

This paper focuses on the simulation of temperature field in automotive dry-clutch

FEA model has been used to predict the temperature rise at frictional interfaces

The roles of the clutch automatic control and of the vehicle dynamics are considered

The results could provide very useful issues to automotive transmission designers

Simulation of engagement control in automotive dry-clutch and temperature field analysis through finite element model

Mario Pisaturo*, Adolfo Senatore

*Department of Industrial Engineering
University of Salerno
84084 Fisciano, Italy*

Abstract

The tribological contact under sliding condition in the clutch facing surfaces during the engagement manoeuvre is strongly affected by heat transfer occurring in the system. The frictional forces acting on the contact surfaces produce mechanical energy losses which are converted in heat with ensuing temperature increase. Reports about the temperature rise after repeated clutch engagements prove the occurrence of interface temperature peaks as high as 300 °C. Unfortunately, only few papers address their focus toward experiments and their outcomes about the influence of temperature and the other operating parameters on the frictional behaviour of the clutch facing materials.

In this paper, the Authors mainly explored the frictional behaviour modification for thermal level higher than 250 – 300 °C, whose effect is a sharp decline of the friction coefficient related to the decomposition of the phenol resin of the facings. Moreover, this phenomenon induces not expected transition from dry friction to mixed dry-lubricated friction which explains the reasons of the friction coefficient drop. The temperature affects also the cushion spring load-deflection characteristic and the ensuing transmitted clutch torque. Thus, an original frictional map has been implemented in a control algorithm to estimate the heat flux during vehicle launch and up-shift

*Corresponding author

Email addresses: mpisaturo@unisa.it (Mario Pisaturo), a.senatore@unisa.it (Adolfo Senatore)

manoeuvres. The results of the longitudinal vehicle dynamics has been used in a FEA to predict the temperature field during repeated clutch engagement on the contact surfaces. The simulation results prove that during each engagement the interface temperature increases of 30 – 35 °C. This means that after only few repeated clutch engagements the temperature field could reach values near the critical point of 300 °C. In such a way, this paper aims at providing useful references to control engineers in order to improve the dry-clutch transmissions performances.

Keywords: dry-clutch, friction coefficient, temperature, finite element analysis, engagement driving

1. Introduction

2 Dry-clutch systems are used in a wide range of applications and one of
3 the most important is the automotive industry. The aim of an automotive
4 dry-clutch is to transfer the torque from the engine to the car wheels. In
5 fact, when the clutch facings are in contact with the pressure plate on one
6 side and the flywheel on the other side, by means of frictional phenomenon,
7 the engine torque flows toward gearbox primary shaft and finally to the car
8 wheels. In this application, as in the automotive brakes application, it is
9 very important to have a high friction coefficient in order to maximize the
10 effectiveness of the system. On the other hand, this means that during normal
11 working conditions there is a noteworthy amount of kinetic energy converted
12 into heat that ensue a temperature increase. The magnitude of temperature
13 rise depends on thermal properties of the clutch facings [1]. This effect is
14 amplified if the system is undergone to repeated load cycles like repeated
15 clutch engagement or repeated breaks in a short time. These situations are
16 very commonly if we consider that every day many drivers spend some hours
17 in the traffic to go and come from work. The main problem is that the friction
18 coefficient of the clutches and brakes linings drops off with the temperature
19 reducing the functionality of the system. In fact, the heat generated may lead
20 to a thermal decomposition of the frictional materials by producing fluids and
21 gas, [2, 3, 4]. Another drawback of this phenomenon is the smell produced
22 with the thermal decomposition of the phenolic resin perceived by the car
23 passengers. In fact, it is one of the main claim to the assistance service.
24 Reports about the temperature rise after repeated clutch engagements prove
25 the occurrence of interface temperature peaks as high as 300 °C [5] and [6].

26 In [7] the Authors have studied the temperature field in automotive dry-
27 clutch during single and repeated engagements under two different hypoth-
28 esis: uniform pressure and uniform wear. The same Authors have analysed
29 the effect of groove pattern and groove size on the temperature field and
30 thermal energy in [8, 9] and the surface temperature distribution of the dry
31 friction clutch system by showing the effect of torque-time variation and
32 dimensionless thickness of the pressure plate in [10].

33 In [11] the FEA analysis has been proposed to predict the facing wear as
34 function of the contact pressure. In [12] a study to estimate the temperature
35 distribution as function of the time and radius during the entire shifting
36 process in dry clutch has been proposed.

37 Adamowicz and Grześ in [13] proposed a three-dimensional FEM to study
38 and compare the temperature distributions caused by mutual sliding of two
39 members of a disc brake system. They assumed that the rotor is subject to
40 the non-axisymmetric thermal load to simulate realistic thermal behaviour
41 of the brake action. They studied also the impact of convective mode of heat
42 transfer on the thermal behaviour of a disc brake system during repetitive
43 braking process with the constant velocity using fully three-dimensional finite
44 element model [14].

45 Finally, in [15] a study on the thermal behaviour of the full and ventilated
46 brake discs of the vehicles has been analysed.

47 Usually, in literature to estimate the heat flux in a dry-clutch during the
48 engagement manoeuvres a linear profile for the sliding angular speed is as-
49 sumed [7, 10]. In this work to accurately estimate the heat flux in a dry-clutch
50 during the engagement manoeuvres, start-up and gear-shift, the vehicle lon-
51 gitudinal dynamics has been considered. In particular, typical manoeuvres
52 have been evaluated and implemented in a suitable control strategy based on
53 the multiple Model Predictive Control (mMPC) designed to track reference
54 trajectories both for the engine and clutch angular speed [16]. Moreover, the
55 controller takes into account the actuator and engine dynamics [17, 18] and
56 a detailed dry-clutch behaviour [19]. To this aim, an original frictional map
57 has been implemented in a control algorithm to estimate the heat flux dur-
58 ing vehicle launch and up-shift manoeuvres. The results of the longitudinal
59 vehicle dynamics has been used in a FEA to predict the temperature field
60 during repeated clutch engagement on the contact surfaces. In the proposed
61 FE model the clutch facing material and the pressure plate have been mod-
62 elled to get the temperature distribution due to the frictional energy. The
63 simulation results prove that after repeated clutch engagements the temper-

64 ature field reaches values near the critical point of 300 °C. In such a way,
65 this paper aims at providing useful references to control engineers in order
66 to improve the dry-clutch transmissions performances.

67 **2. Dry-clutch system**

68 The aim of this section is to clarify the role of the main variables that
69 explicitly influence the transmissibility of a dry-clutch system. The analy-
70 sis of functional and structural links between the clutch engagement system
71 and other driveline components is the first fundamental step for solving the
72 modelling issues [20]. Recent studies have shown that the availability of phe-
73 nomenological model of the torque transmissibility implemented in the TCU
74 is fundamental to improve the performances of the automated dry-clutch.
75 Until now the control strategies implemented in the TCUs take into account
76 a simplified model of the friction phenomena and without considering the
77 operation of clutch subsystems [21]. Indeed, these latter have a remarkable
78 influence on the shifting quality of the gear shifts and consequently on the
79 performances of the automated transmission. By describing a typical engage-
80 ment process it has been illustrated how the diaphragm spring [22, 23, 24]
81 and the cushion spring [25, 26] take part in the transmissibility character-
82 istic. Even though the torque transmitted through a dry-clutch influences
83 and is influenced by driveline components and diaphragm spring, the torque
84 transmissibility proposed model shows that the two main elements to be
85 considered are the cushion spring load and the dry friction phenomenon. In
86 the next subsections, how these two elements enter separately into the pro-
87 posed torque transmissibility model is shown. In such model the influence of
88 the temperature [2, 5, 27, 28], of the slip speed and of the contact pressure
89 [29, 30, 19] has been taken into account. Finally a novel torque transmissi-
90 bility model of the automated dry-clutch such as AMT and DCT has been
91 defined. In Figure 1 the dry-clutch architecture is showed.

92 *2.1. Friction coefficient*

93 The friction coefficient has a strong effect on the clutch torque character-
94 istic as it is shown in the next paragraphs. For this reason a deep analysis
95 on its variation during the engagement phase is fundamental to improve the
96 performance of an actuated dry-clutch. The modelling of friction variation
97 during the clutch engagement process has been studied by numerous authors.

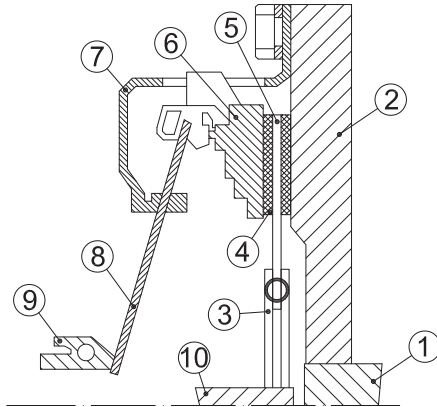


Figure 1: Dry-clutch architecture: 1 crank-shaft, 2 flywheel, 3 clutch disc, 4 clutch facings, 5 cushion spring, 6 pressure plate, 7 cover, 8 diaphragm spring, 9 throwout bearing, 10 primary shaft

98 In this section is explained how the temperature, the sliding speed and
 99 average contact pressure affect the friction coefficient. In [30, 19] a detailed
 100 analysis is reported therefore for the sake of brevity here are highlighted only
 101 the main results.

102 In Figure 2 the technical data sheet of a typical automotive clutch fac-
 103 ings is showed [27]. In that graph the friction coefficient exhibits a smooth
 104 variation within the temperature range from 100 °C to 250 °C, whereas it
 105 begins to sharply decline above 250 °C. This typical behaviour is also shown
 106 in [2, 3]. This effect is related to the decomposition of the phenolic resin of
 107 the clutch facings at higher temperature. In fact, when the temperature is
 108 higher than 330 °C, a severe thermal decomposition produces fluids and gas
 109 emissions. This effect induces not expected transition phenomena from dry
 110 friction to lubricated friction. For this reason the friction coefficient drops
 111 [2, 3].

112 Instead, in Figure 3 is pointed out the relationship between the friction
 113 coefficient and the sliding speed for two different average contact pressures,
 114 [30]. It is evident that for both contact pressure level the friction coefficient
 115 tends to an asymptotic value at higher sliding speeds. The friction coefficient
 116 asymptotic value is higher for higher contact pressure. Moreover, the contact
 117 pressure has a nearly linear influence on the friction coefficient, according to
 118 the results in [30], achieved on a tribometer at room temperature, Figure 3.

119 Thus, the dependence of the friction coefficient on sliding speed, average

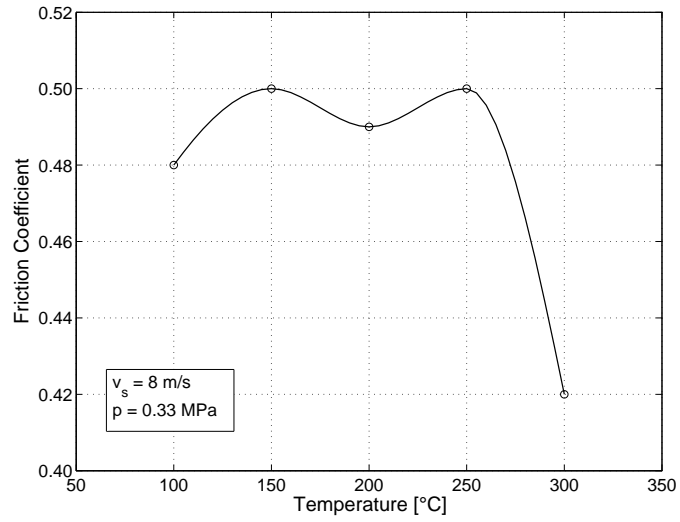


Figure 2: Friction coefficient vs. average facing temperature, [27]

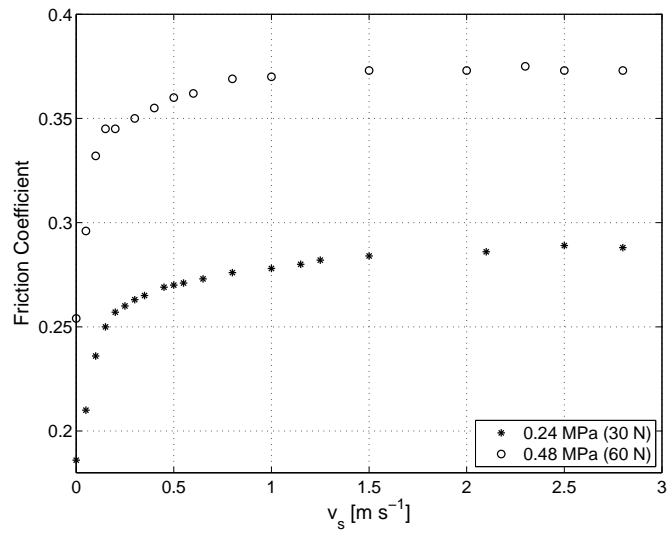


Figure 3: Friction coefficient vs. sliding speed at different contact pressure: 0.24 MPa, 0.48 MPa, [30]

120 contact pressure and facing temperature is given by the equations (1) and
 121 (2):

$$\mu_{\infty}(p, \theta_{cm}) = \alpha + \beta \frac{p}{p_0} + f(\theta_{cm}) \quad (1)$$

122 where α and β have been identified from the Figure 3 in the plateau region
 123 and the corresponding values are: $\alpha = -0.110$, $\beta = 0.110$; the reference
 124 pressure is $p_0 = 0.33 \text{ MPa}$, i.e. the same average contact pressure of the
 125 experiments in Figure 2, [27]. The function f is derived from the data in
 126 Figure 2.

127 The equation (2) is based on the experimental results in [30] for strictly
 128 positive slip speed:

$$\mu(v_s, p, \theta_{cm}) = \mu_{\infty}(p, \theta_{cm}) + \mu_{\Delta} \left(\tanh\left(\frac{v_s}{v^*}\right) - 1 \right) \quad (2)$$

129 In equation (2), $v_s = R_m |\omega_e - \omega_c|$ is the sliding speed given by the product
 130 between the difference between engine and clutch angular speed $|\omega_e - \omega_c|$
 131 and mean radius R_m . μ_{Δ} and v^* have been identified and the corresponding
 132 values are 0.09 and 0.5 m/s, respectively.

133 2.2. Cushion spring

134 The cushion spring is a thin steel disc placed between the clutch friction
 135 pads and is designed with different radial stiffness in order to ensure the
 136 desired smoothness of engagement [21]. When the cushion spring is com-
 137 pletely compressed by the pressure plate we say that the clutch is *closed*,
 138 whereas when the pressure plate position is such that the cushion spring is
 139 not compressed we say that the clutch is *open*. We say that the clutch is in
 140 the slipping phase when is going from open to locked-up, i.e. the flywheel
 141 and the clutch disc have the same angular speed $\omega_e = \omega_c$. The tempera-
 142 ture influences the cushion spring load-deflection characteristic [26] and this
 143 latter influences the clutch torque transmissibility. In [28] a detailed finite
 144 element analysis has been carried out in order to evaluate the influence of
 145 the temperature on the cushion spring characteristic, Figure 4.

146 2.3. Transmissibility model

147 By considering the results shown in the previous subsections on the cush-
 148 ion spring and on the friction coefficient it has been developed a more complex
 149 clutch torque transmissibility model reported in the equation (3), [19].

$$T_{fc}(y, \theta_{cs}, \theta_{cm}, v_s, p) = n\mu(v_s, p, \theta_{cm})R_m F_{fc}(\delta_f(x_{pp}(y, \theta_{cs}), \theta_{cs})) \quad (3)$$

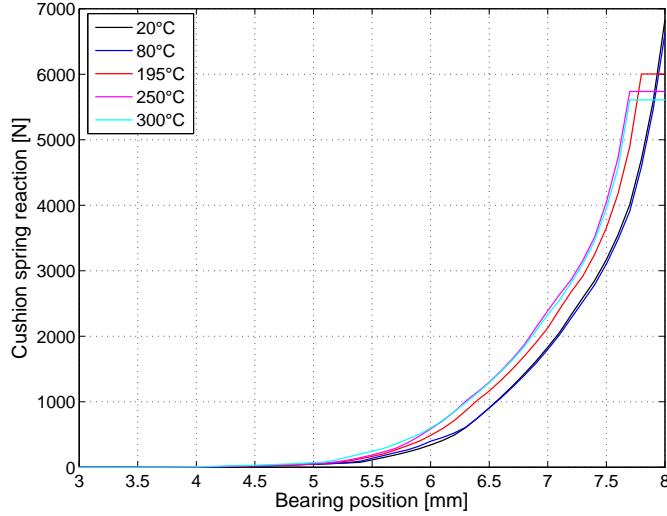


Figure 4: Cushion spring characteristic at increasing temperature levels, [28]

150 where T_{fc} is the torque transmitted by the clutch, $R_m = \frac{2}{3} \frac{R_e^3 - R_i^3}{R_e^2 - R_i^2}$ is a geo-
 151 metrical parameter obtained under the assumption of a uniform pressure, y
 152 is the throwout bearing position, θ_{cs} and θ_{cm} are the cushion spring and the
 153 clutch material temperature respectively, F_{fc} is the cushion spring reaction.
 154 This model has been implemented in a control algorithm in order to describe
 155 the behaviour of the dry-clutch architecture.

156 3. Heat flux estimation

157 As mentioned in the paragraph 1, in this work to accurately estimate the
 158 heat flux in a dry-clutch during the engagement manoeuvres, the vehicle lon-
 159 gitudinal dynamics has been considered. In particular, typical manoeuvres
 160 have been evaluated and implemented in a suitable control strategy based
 161 on the multiple Model Predictive Control (mMPC) [16] which take into ac-
 162 count the actuator and engine dynamics [17, 18] and a detailed dry-clutch
 163 behaviour [19]. For the sake of brevity the equations that describe the vehicle
 164 longitudinal dynamics are omitted but a detailed mathematical representa-
 165 tion can be found in the cited literature. In Figure 5 the control scheme
 166 implemented in MATLAB/Simulink has been reported. The heat flux esti-
 167 mated with this approach has been used into a FEM model to calculate the

168 temperature field in the dry-clutch components.

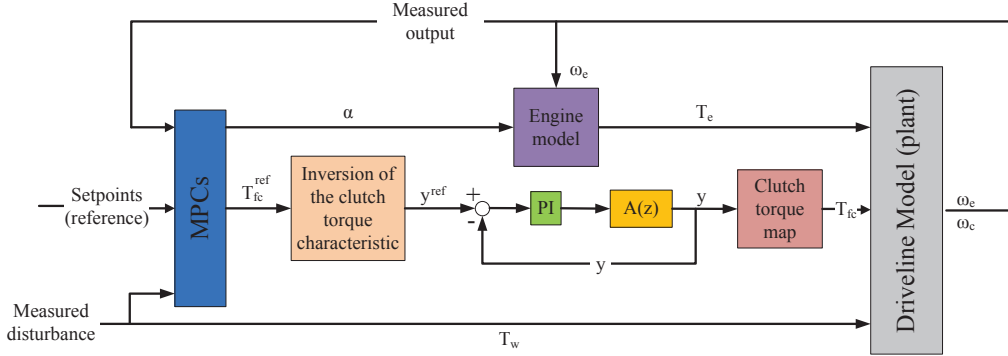


Figure 5: Control scheme

169 In particular has been simulated three different manoeuvres, both vehicle
 170 launches and gear-shift, to estimate the heat flux in each working condition.
 171 The aim is to evaluate how the thermal power Q varies with the time by using
 172 the outputs of the control algorithm, namely the angular sliding speed ω_{sl}
 173 and the frictional torque transmitted by the clutch during the manoeuvre
 174 T_{fc} . By assuming that all the frictional work is converted into heat, the
 175 thermal power during the clutch engagement is given by:

$$Q(t) = T_{fc}(t) \omega_{sl}(t) \quad (4)$$

176 Finally, by considering the contact surface equal to the interface geomet-
 177 rical surface the heat flux has been evaluated.

178 3.1. Manoeuvre 1

179 In this subsection the plots of the main results concerning a vehicle launch
 180 manoeuvre are reported. In Figure 6 the engine, clutch and sliding angular
 181 speed have been reported.

182 Instead, Figure 7 shows the frictional torque transmitted by the clutch
 183 during the engagement manoeuvre.

184 As explained previously the frictional work converted into heat, and con-
 185 sequently the thermal power, generated during the clutch engagement have
 186 been estimate by the equation (4) by using the values highlighted in the
 187 above figures. In Figure 8 the thermal power and the heat flux due to the
 188 simulated start-up manoeuvre have been plotted.

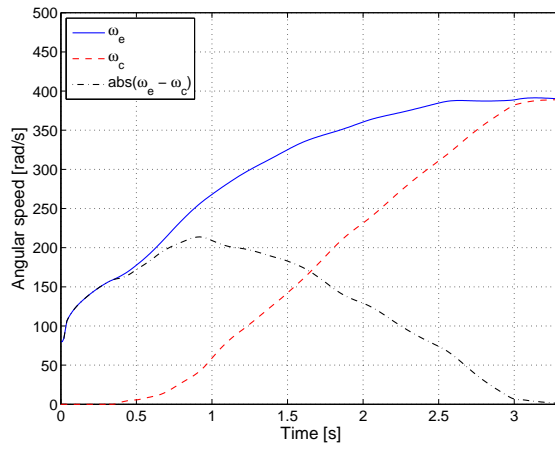


Figure 6: Manoeuvre 1 - Angular speeds

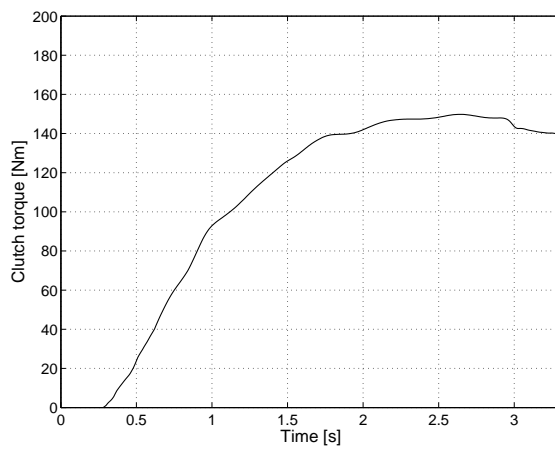


Figure 7: Manoeuvre 1 - Clutch torque

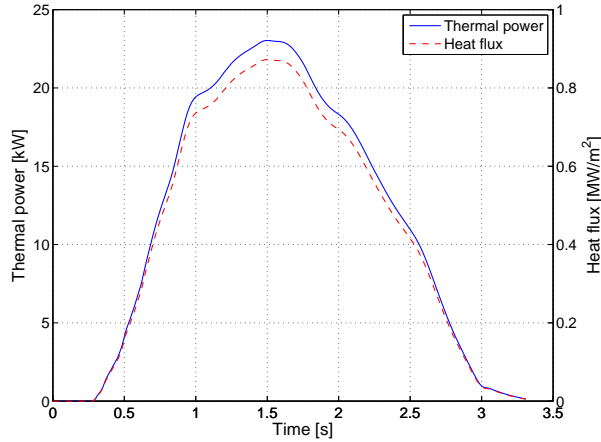


Figure 8: Manoeuvre 1 - Thermal power and heat flux

189 *3.2. Manoeuvre 2*

190 In this subsection another vehicle launch manoeuvre has been analysed
 191 in the same way explained above. In Figure 9 the engine, clutch and sliding
 192 angular speed have been reported. It is worth to note that in this case the
 193 engine angular speed increases suddenly in the first half second by resulting in
 194 a higher sliding speed and consequently in a higher thermal power generated
 195 during the manoeuvre respect to the previous one.

196 Instead, Figure 10 shows the frictional torque transmitted by the clutch
 197 during the engagement manoeuvre.

198 As explained previously the frictional work converted into heat, and con-
 199 sequently the thermal power, generated during the clutch engagement have
 200 been estimate by the equation (4) by using the values highlighted in the
 201 above figures. In Figure 11 the thermal power and the heat flux due to the
 202 simulated start-up manoeuvre have been pointed out.

203 *3.3. Manoeuvre 3*

204 Finally, a vehicle launch manoeuvre together to an up-shift $1^{st} - 2^{nd}$ has
 205 been considered in order to compare the thermal power generated during
 206 these two different working conditions. In Figure 12 the engine, clutch and
 207 sliding angular speed obtained in this case have been reported. It underlines
 208 that heat generated during the up-shift is negligible. In fact, during a gear-
 209 shift request the transmission control unit gives the command to open the

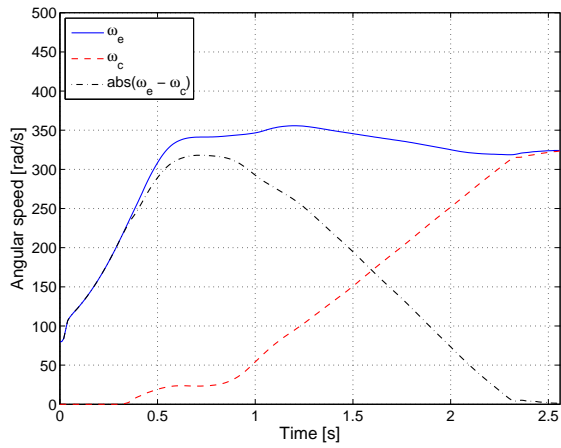


Figure 9: Manoeuvre 2 - Angular speeds

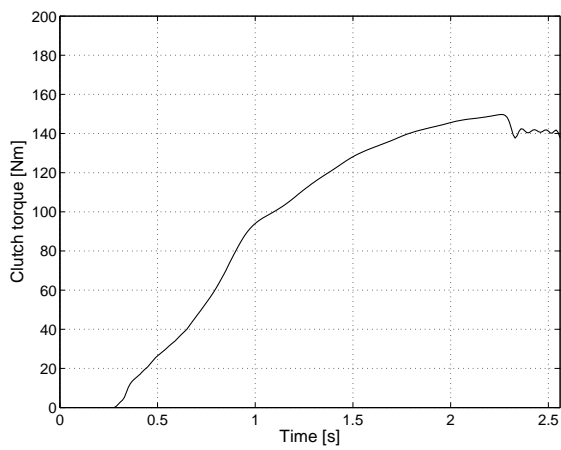


Figure 10: Manoeuvre 2 - Clutch torque

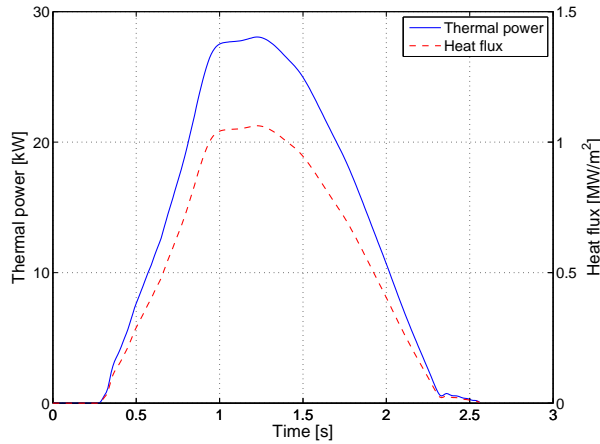


Figure 11: Manoeuvre 3 - Thermal power and heat flux

210 clutch as fast as possible and consequently the clutch torque go to zero. When
 211 the requested gear is engaged and the synchronization phase is completed the
 212 clutch speed disc moves quickly the speed value corresponding to the vehicle
 213 speed reported to the main-shaft through the new gear ratio [31].

214 Instead, Figure 13 shows the frictional torque transmitted by the clutch
 215 during the manoeuvre.

216 In Figure 14 the thermal power and the heat flux due to the simulated
 217 start-up manoeuvre have been plotted.

218 4. FE model

219 To appraise the interface temperature during the engagement manoeuvres
 220 a Finite Element Model (FEM) has been implemented by using a commercial
 221 software. In particular, by considering the axisymmetric of the system a 2D-
 222 model has been considered in the numerical simulations. In Figure 15 the
 223 clutch system which has been taken into account is reported. The values
 224 obtained from the simulations take into account the total amount of the heat
 225 generated during the manoeuvres, i.e. on both the contact pairs surfaces.
 226 But, in the proposed 2D-model only one contact pair is analysed. Thus,
 227 by considering the symmetry on the mid-plane the hypothesis that in each
 228 contact pair is generated the 50% of the total heat has been made. Under
 229 this latter consideration a thermal symmetry condition has been imposed on

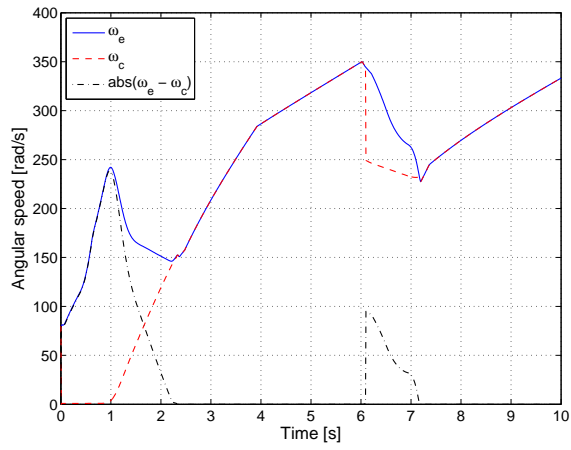


Figure 12: Manoeuvre 3 - Angular speeds

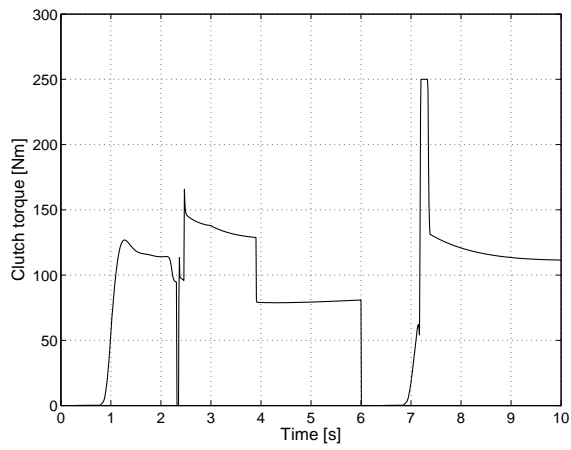


Figure 13: Manoeuvre 3 - Clutch torque

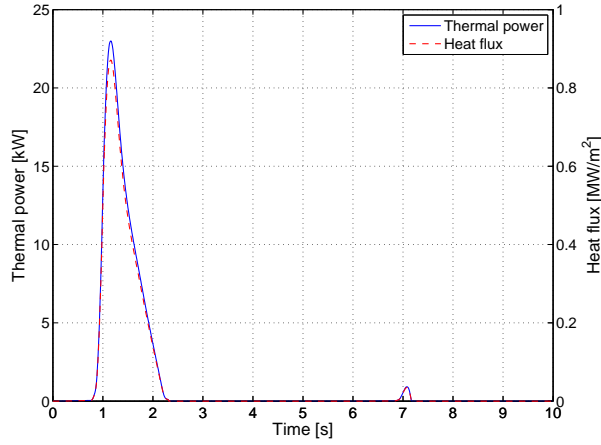


Figure 14: Manoeuvre 3 - Thermal power and heat flux

230 the mid-plane, Figure 15. Finally, on all the surfaces in contact with the air
 231 conductive losses, by using a conductive coefficient of $20 \text{ Wm}^{-2}\text{K}^{-1}$ and a
 232 bulk temperature of 298 K , have been imposed. So, only conduction and
 233 convection thermal mechanism has been considered in this paper. In fact,
 234 due to the short time and the relatively low temperatures reached during the
 235 engagement it is possible to neglect the radiant phenomenon.

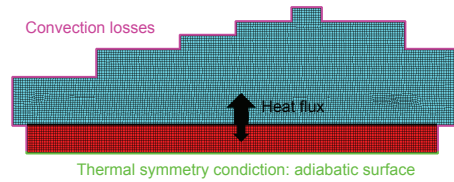


Figure 15: Finite element model

236 As mentioned before, a uniform contact pressure between the clutch disc
 237 and the pressure plate has been considered to calculate the frictional work
 238 converted into heat. This means that the heat flux is independent from the
 239 spatial distribution. Furthermore, it was assumed that the heat flows in
 240 a direction perpendicular to the contact surfaces. The heat partition ratio
 241 has been calculate with the Charron's formula recommended for brakes and
 242 clutches applications [32], eq. (5):

$$\gamma = \frac{\sqrt{K_1 \rho_1 C_1}}{\sqrt{K_1 \rho_1 C_1} + \sqrt{K_2 \rho_2 C_2}} \quad (5)$$

243 where K is the thermal conductivity, ρ the density and C the specific
 244 heat capacity. The subscribes 1 indicate the clutch disc and 2 the pressure
 245 plate respectively. The heat partition ratio has been calculate by considering
 246 the materials proprieties of both the bodies isotropic and independent from
 247 the temperature. In Table 1 the materials proprieties used for the numerical
 248 analysis are listed:

Table 1: Material proprieties

Parameters	Pressure plate	clutch disc
Density [kgm^{-3}]	7250	1540
Young's module [GPa]	150	3.68
Poisson ratio	0.28	0.25
Thermal conductivity [$Wm^{-1}K^{-1}$]	48	0.70
Specific heat capacity [$Jkg^{-1}K^{-1}$]	540	750
Linear expansion [K^{-1}]	10^{-5}	$16 \cdot 10^{-6}$

249 5. Simulation Results

250 In this paragraph the results of the numerical simulation described be-
 251 fore are reported. In particular, the goal of this paper is to estimate the
 252 temperature increase after repetitive engagements for each manoeuvre which
 253 could represent urban traffic scenario. To this aim each manoeuvre has been
 254 repeated in order to cover a window time of about 40 s. Details on the load
 255 cycle considered in each case are explained in the dedicated subsection.

256 5.1. Manoeuvre 1

257 In Figure 16 the interface temperature and the temperature on the cush-
 258 ion spring side versus time at different radii are plotted. The picture high-
 259 lights also the single load cycle which has a first part that represents the
 260 slipping phase of 3.45 s and a second part of 5 s which represent the engaged
 261 phase. The same load cycle has been repeated 5 times to cover the window
 262 time considered. This picture shows how the interface temperature (solid
 263 lines) rises during the first part of the slipping phases (about 30 – 35 K)

264 and it decreases during the engaged phases under the effect of the convective
 265 losses. The results highlight that the convective losses can not dissipate com-
 266 pletely the thermal energy generated during the slipping phase. Moreover,
 267 after only five repeated engagements the interface temperature can attain
 268 about $430 - 450\text{ K}$, i.e. about $160 - 180\text{ }^\circ\text{C}$, near the critical temperature
 269 value for clutch materials [6, 2]. The temperature on the cushion spring side
 270 (dashed lines) presents a behaviour smoother than the interface temperature
 271 due to the effect of the clutch material thickness. In any case, it is worth
 272 noting that after repeated engagements also on the cushion spring side it is
 273 possible to attain high temperature. This results in a change of the cushion
 274 spring load-deflection characteristic as showed in the section 2.

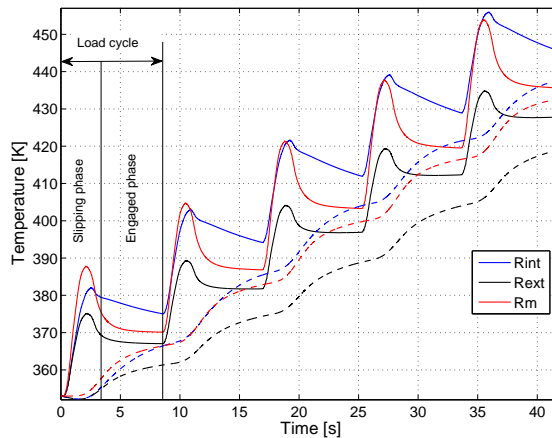


Figure 16: Manoeuvre 1 - Interface Temperatures (solid lines) and cushion spring side (dashed lines) vs. time after repeated engagements

275 The differences between the temperatures at different radii are due to
 276 the irregular geometry of the pressure plate which results in a non-uniform
 277 temperature distribution, Figure 17. Indeed, on the external radius the tem-
 278 perature increase is lower than on the internal and medium radii due to the
 279 irregular geometry of the pressure plate. Indeed, this latter presents in the
 280 internal zone a reduced thickness that results in a higher cumulated thermal
 281 energy during each load cycle that the convective losses can not dissipate
 282 completely.

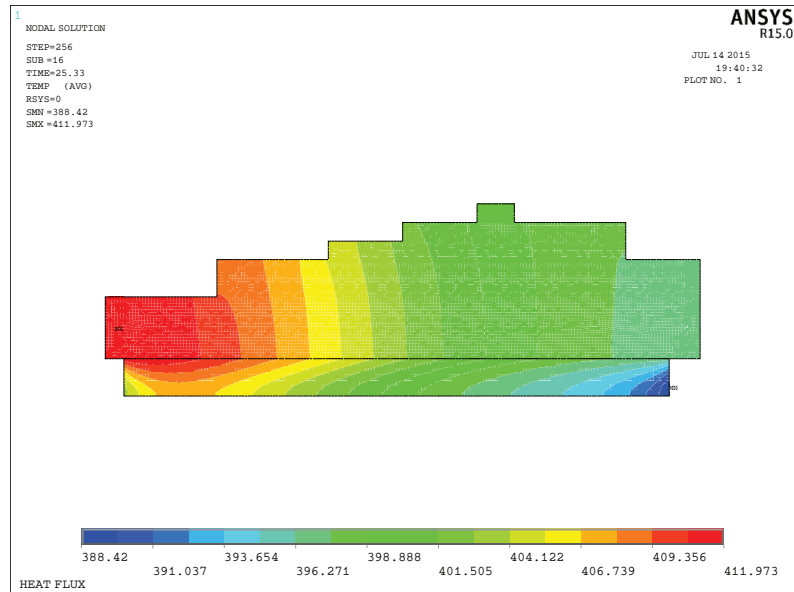


Figure 17: Manoeuvre 1 - Temperature distribution at time step 25.3 s

283 *5.2. Manoeuvre 2*

284 In Figure 18 the interface temperature and the temperature on the cushion
 285 spring side versus time at different radii are plotted for the second ma-
 286 noeuvre. In this case the slipping phase is of 2.70 s and the engaged phase
 287 is of 5 s. Also in this simulation the same load cycle has been repeated 5
 288 times to cover the window time considered. As explained previously during
 289 this manoeuvre the frictional work converted into heat is higher than previ-
 290 ous one, so in this case the interface temperature rises of about 30 – 40K.
 291 The behaviour of the temperature on both sides of the clutch materials dur-
 292 ing the engaged phases is the same observed for the manoeuvre 1. Indeed,
 293 also these results highlight that the convective losses can not dissipate com-
 294 pletely the thermal energy generated during the slipping phase. Moreover,
 295 after only five repeated engagements the interface temperature can attain a
 296 temperature close to the critical value for clutch materials.

297 *5.3. Manoeuvre 3*

298 Finally, the third manoeuvre represents a vehicle launch and an up-shift
 299 and as underlined above the heat generated during the up-shift is negligible.

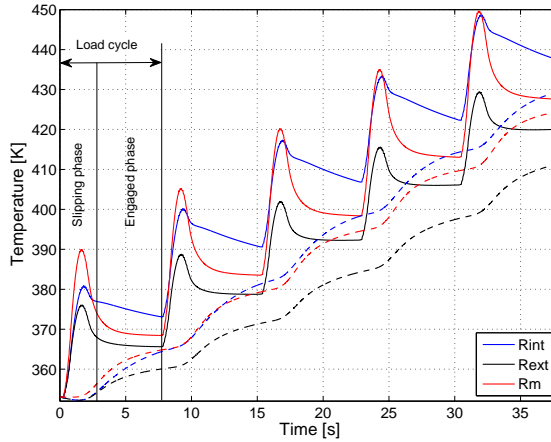


Figure 18: Manoeuvre 2 - Interface Temperatures (solid lines) and cushion spring side (dashed lines) vs. time after repeated engagements

300 For these reasons during a gear-shift manoeuvre the generated heat is neg-
 301 ligible and in the load cycle reported in Figure 19 the temperature increase
 302 due to the up-shift is practically zero. For this manoeuvre the frictional work
 303 converted into heat is lower than the previous cases and concentrated in a
 304 short time. This results in a temperature increase lower than the manoeuvres
 305 reported previously. Moreover, as highlighted in Figure 19 the interface
 306 temperature and the temperature on the cushion spring side versus time at
 307 different radii have the same trend discussed above.

308 6. Concluding Remarks

309 By concluding, in this paper three typical vehicle launch manoeuvres have
 310 been analysed to estimate the heat flux due to the friction phenomenon in a
 311 dry-clutch assembly. These results have been used to set up an axisymmetric
 312 finite element model of a clutch facing in contact with the pressure plate. The
 313 aim of the FE analysis is to calculate the temperature increase after repeated
 314 clutch engagements. The simulation results have showed that during each
 315 slipping phase the temperature increase can reach about 30 – 35 K . On the
 316 other hand, during the engaged phase the convective losses cannot dissipate
 317 completely this thermal energy. Moreover, after only 5 repeated engagements
 318 the interface temperature can amount to about 430 – 450 K . Namely, the
 319 thermal load in these working conditions could lead to critical temperature

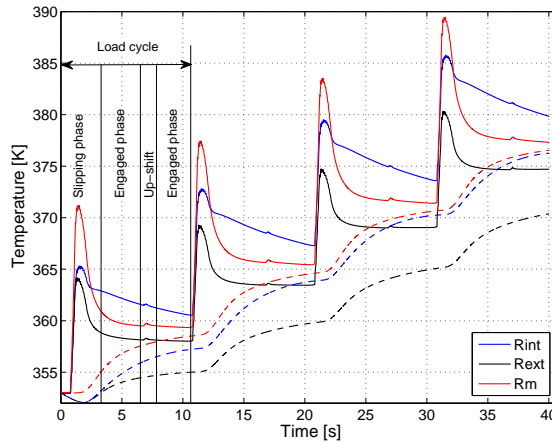


Figure 19: Manoeuvre 2 - Interface Temperatures (solid lines) and cushion spring side (dashed lines) vs. time after repeated engagements

320 values after few repeated engagements. This means that the clutch facings
 321 could suffer permanent damages together with smell perceived by the car
 322 passengers and a reduction of the performances.

323 References

- 324 [1] A. Khamlichi, M. Bezzazi, A. Jabbouri, P. Reis, J. P. Davim, Opti-
 325 mizing Friction Behaviour of Clutch Facings Using Pin-on-Disk Test,
 326 International Journal of Physical Sciences 3 (2008) 65–70.
- 327 [2] H. Feng, M. Yimin, L. Juncheng, Study on Heat Fading of Phenolic
 328 Resin Friction Material for Micro-automobile Clutch, in: Measuring
 329 Technology and Mechatronics Automation (ICMTMA), 2010 Interna-
 330 tional Conference on, Vol. 3, 2010, pp. 596–599.
- 331 [3] A. Yevtushenko, A. Adamowicz, P. Grześ, Three-dimensional {FE}
 332 Model for the Calculation of Temperature of a Disc Brake at
 333 Temperature-dependent Coefficients of Friction, International Commu-
 334 nications in Heat and Mass Transfer 42 (0) (2013) 18–24.
- 335 [4] L. Wawrzonek, R. A. Biaiecki, Temperature in a disk brake, simulation
 336 and experimental verification, International Journal of Numerical Meth-
 337 ods for Heat & Fluid Flow 18 (3/4) (2008) 387–400.

- 338 [5] B. Czél, K. Váradi, A. Albers, M. Mitariu, FE Thermal Analysis of a
339 Ceramic Clutch, *Tribology International* 42 (5) (2009) 714–723.
- 340 [6] Kimming, Agner, Double Clutch: Wet or Dry, this is the question
341 (2006).
- 342 [7] O. Abdullah, J. Schlattmann, Finite element analysis of temperature
343 field in automotive dry friction clutch, *Tribology in Industry* 34 (4)
344 (2012) 206–216.
- 345 [8] O. Abdullah, J. Schlattmann, Finite Element Analysis for Grooved Dry
346 Friction Clutch, *Advances in Mechanical Engineering and its Applica-*
347 *tions* 2 (1) (2012) 121–133.
- 348 [9] O. Abdullah, J. Schlattmann, Finite Element Analysis of Dry Friction
349 Clutch With Radial and Circumferential Grooves, in: *Proceedings of*
350 *the World Academy of Science, Engineering and Technology Conference,*
351 *Paris, France, 2011,* pp. 1279–1291.
- 352 [10] O. Abdullah, J. Schlattmann, Computation of Surface Temperatures
353 and Energy Dissipation in Dry Friction Clutches for Varying Torque with
354 Time, *International Journal of Automotive Technology* 15 (5) (2014)
355 733–740.
- 356 [11] S. Sfarni, E. Bellenger, J. Fortin, M. Malley, Numerical and experimental
357 study of automotive riveted clutch discs with contact pressure analysis
358 for the prediction of facing wear, *Finite Elem. Anal. Des.* 47 (2) (2011)
359 129–141.
- 360 [12] Y. Wang, Y. Li, N. Li, H. Sun, C. Wu, T. Zhang, Time-varying Fric-
361 tion Thermal Characteristics Research on a Dry Clutch, *Proceedings of*
362 *the Institution of Mechanical Engineers, Part D: Journal of Automobile*
363 *Engineering* 228 (5) (2014) 510–517.
- 364 [13] A. Adamowicz, P. Grześ, Analysis of Disc Brake Temperature Distri-
365 bution During Single Braking Under Non-axisymmetric Load , *Applied*
366 *Thermal Engineering* 31 (67) (2011) 1003 – 1012.
- 367 [14] A. Adamowicz, P. Grześ, Influence of convective cooling on a disc brake
368 temperature distribution during repetitive braking, *Applied Thermal*
369 *Engineering* 31 (1415) (2011) 2177–2185.

- 370 [15] A. Belhocine, M. Bouchetara, Thermal Analysis of a Solid Brake Disc,
371 Applied Thermal Engineering 32 (2012) 59–67.
- 372 [16] M. Pisaturo, M. Cirrincione, A. Senatore, Multiple Constrained
373 MPC Design for Automotive Dry Clutch Engagement, Mechatronics,
374 IEEE/ASME Transactions on 20 (1) (2015) 469–480.
- 375 [17] M. Pisaturo, A. Senatore, V. D’Agostino, N. Cappetti, Model Predic-
376 tive Control for Electro-hydraulic Actuated Dry Clutch in AMT Trans-
377 missions, in: The 14th Mechatronics Forum International Conference,
378 Karlstad, Sweden, 2014, june, 16-18.
- 379 [18] M. Pisaturo, A. Senatore, V. D’Agostino, Model Predictive Control for
380 Actuated Dry-Clutch Management to Reduce Vehicle Launch Delay Due
381 to Engine Torque Build-up, in: International Control Automation Tech-
382 nologies Conference, 2014, october 13.
- 383 [19] V. D’Agostino, M. Pisaturo, A. Senatore, Improving the Engagement
384 Performance of Automated dry Clutch Through the Analysis of the In-
385 fluence of the Main Parameters on the Frictional Map, in: 5th World
386 Tribology Congress, Turin, Italy, 2013, november, 8-13.
- 387 [20] F. Vasca, L. Iannelli, A. Senatore, G. Reale, Torque Transmissibil-
388 ity Assessment for Automotive Dry-Clutch Engagement, Mechatronics,
389 IEEE/ASME Transactions on 16 (3) (2011) 564–573.
- 390 [21] F. Vasca, L. Iannelli, A. Senatore, M. Scafati, Modeling Torque Trans-
391 missibility for Automotive Dry Clutch Engagement, in: American Con-
392 trol Conference, 2008, pp. 306–311.
- 393 [22] S. Mauro, G. Mattiazzo, M. Velardocchia, G. Serra, F. Amisano, G. Er-
394 cole, The Influence of the Push-plate Mechanical Characteristic on
395 Torque Transmissibility in Diaphragm Spring Clutches, in: AIMETA
396 Internationa Tribology Conference, 2002, september, 18-20.
- 397 [23] G. La Rosa, M. Messina, A. Risitano, Stiffness of Variable Thickness
398 Belleville Springs, Journal of Mechanical Design 123 (2) (1998) 294–
399 299.

- 400 [24] N. Cappetti, M. Pisaturo, A. Senatore, Temperature Influence on the
401 Engagement Uncertainty in Dry Clutch-AMT, in: Proceedings of Global
402 Powertrain Congress, Frankfurt, Germany, 2012, may, 9-10.
- 403 [25] S. Sfarni, E. Bellenger, J. Fortin, M. Malley, Finite Element Analysis of
404 Automotive Cushion Discs, *Thin-Walled Structures* 47 (4) (2009) 474–
405 483.
- 406 [26] N. Cappetti, M. Pisaturo, A. Senatore, Modelling the Cushion Spring
407 Characteristic to Enhance the Automated Dry-Clutch Performance:
408 The Temperature Effect, Proceedings of the Institution of Mechanical
409 Engineers, Part D: Journal of Automobile Engineering 226 (11) (2012)
410 1472–1482.
- 411 [27] LuK, Technical Data Sheet for Friction Material R-233.
- 412 [28] V. D’Agostino, N. Cappetti, M. Pisaturo, A. Senatore, Improving the
413 Engagement Smoothness Through Multi-Variable Frictional Map in Au-
414 tomated Dry Clutch Control, in: Proceedings of the ASME2012 Interna-
415 tional Mechanical Engineering Congress & Exposition, Vol. 11, Houston,
416 Texas, USA, 2012, pp. 9–19, november, 9-15.
- 417 [29] C. Duan, R. Singh, Dynamics of a 3DoF Torsional System with a Dry
418 Friction Controlled Path, *Journal of Sound and Vibration* 289 (4-5)
419 (2006) 657–688.
- 420 [30] A. Senatore, V. D’Agostino, R. Di Giuda, V. Petrone, Experimental In-
421 vestigation and Neural Network Prediction of Brakes and Clutch Mate-
422 rial Frictional Behaviour Considering the Sliding Acceleration Influence,
423 *Tribology International* 44 (10) (2011) 1199–1207.
- 424 [31] L. Glielmo, L. Iannelli, V. Vacca, F. Vasca, Gearshift Control for Auto-
425 mated Manual Transmissions, *Mechatronics, IEEE/ASME Transactions*
426 on 11 (1) (2006) 17–26.
- 427 [32] P. Grześ, Partition of Heat in 2D Finite Element Model of a Disc Brake,
428 *Acta Mechanica et Automatica* 5 (2011) 35–41.

Fig. 1

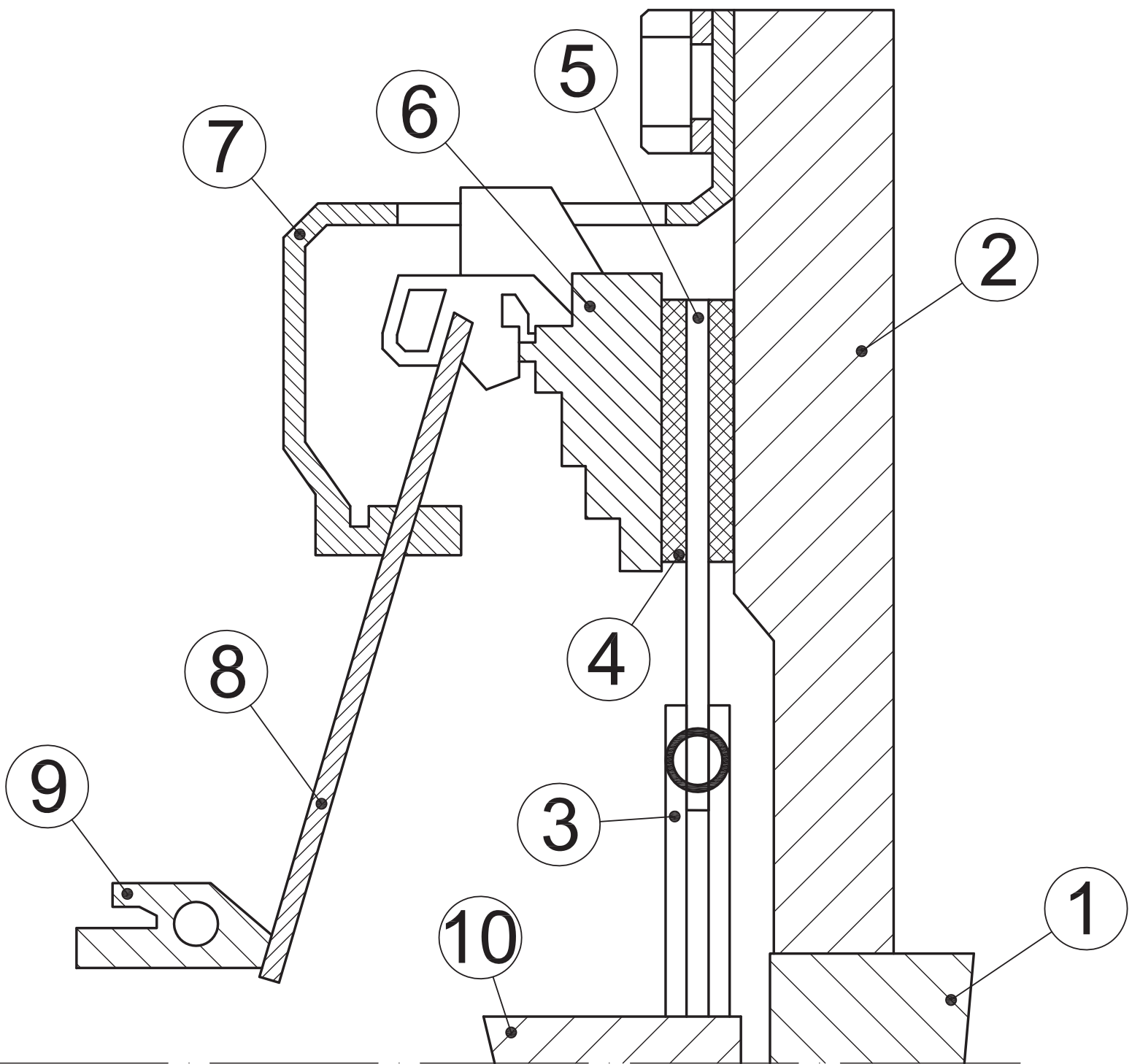


Fig. 2

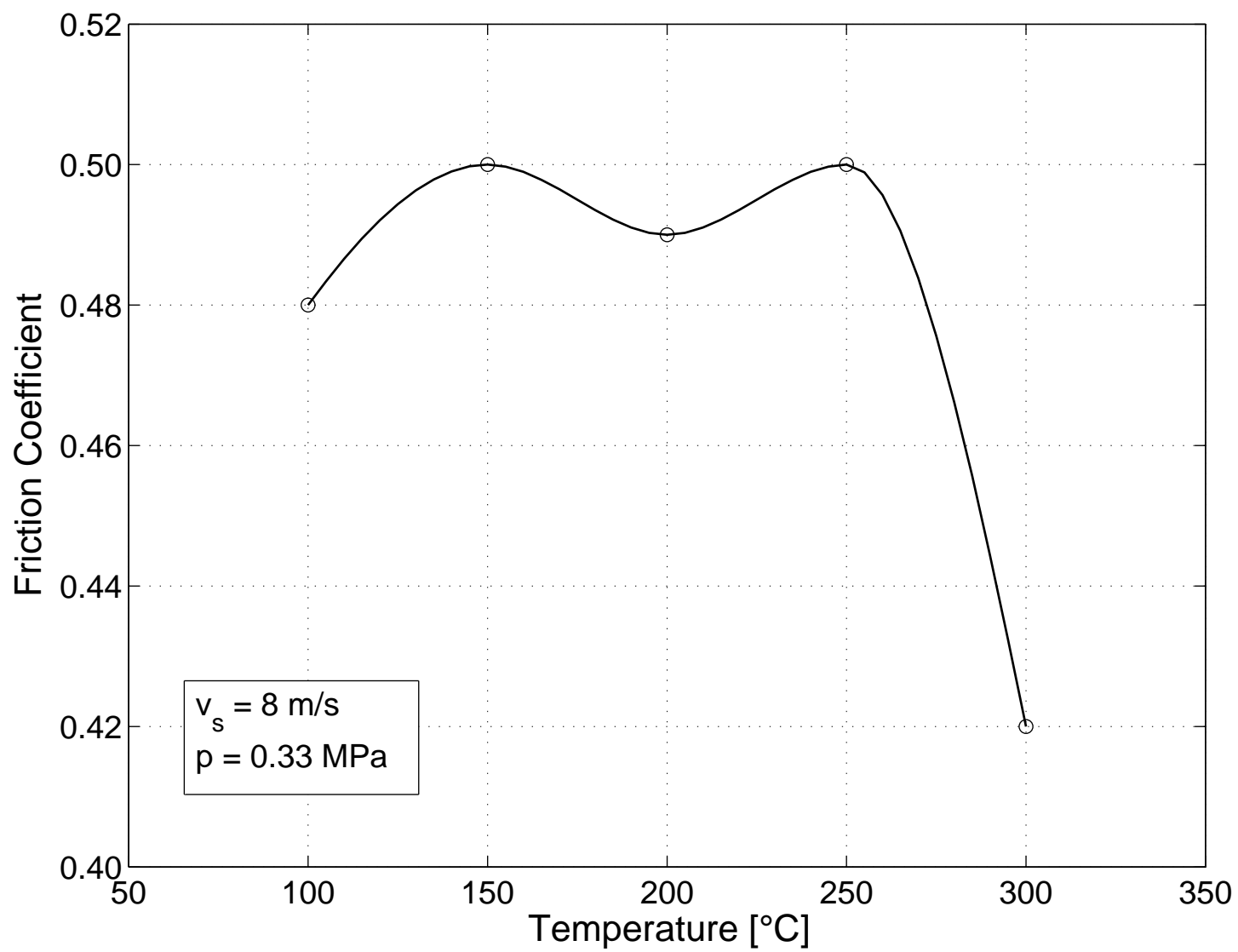


Fig. 3

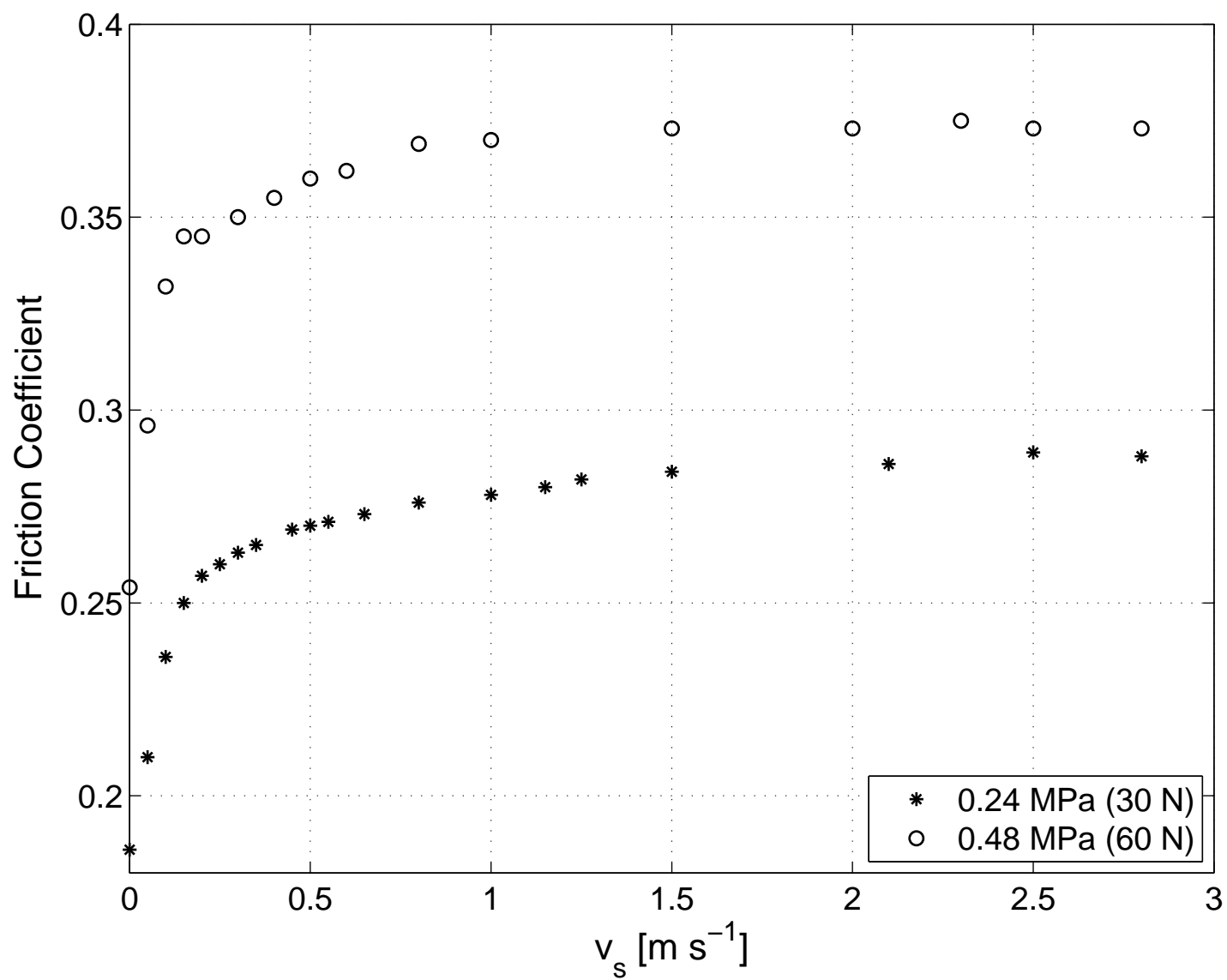


Fig. 4

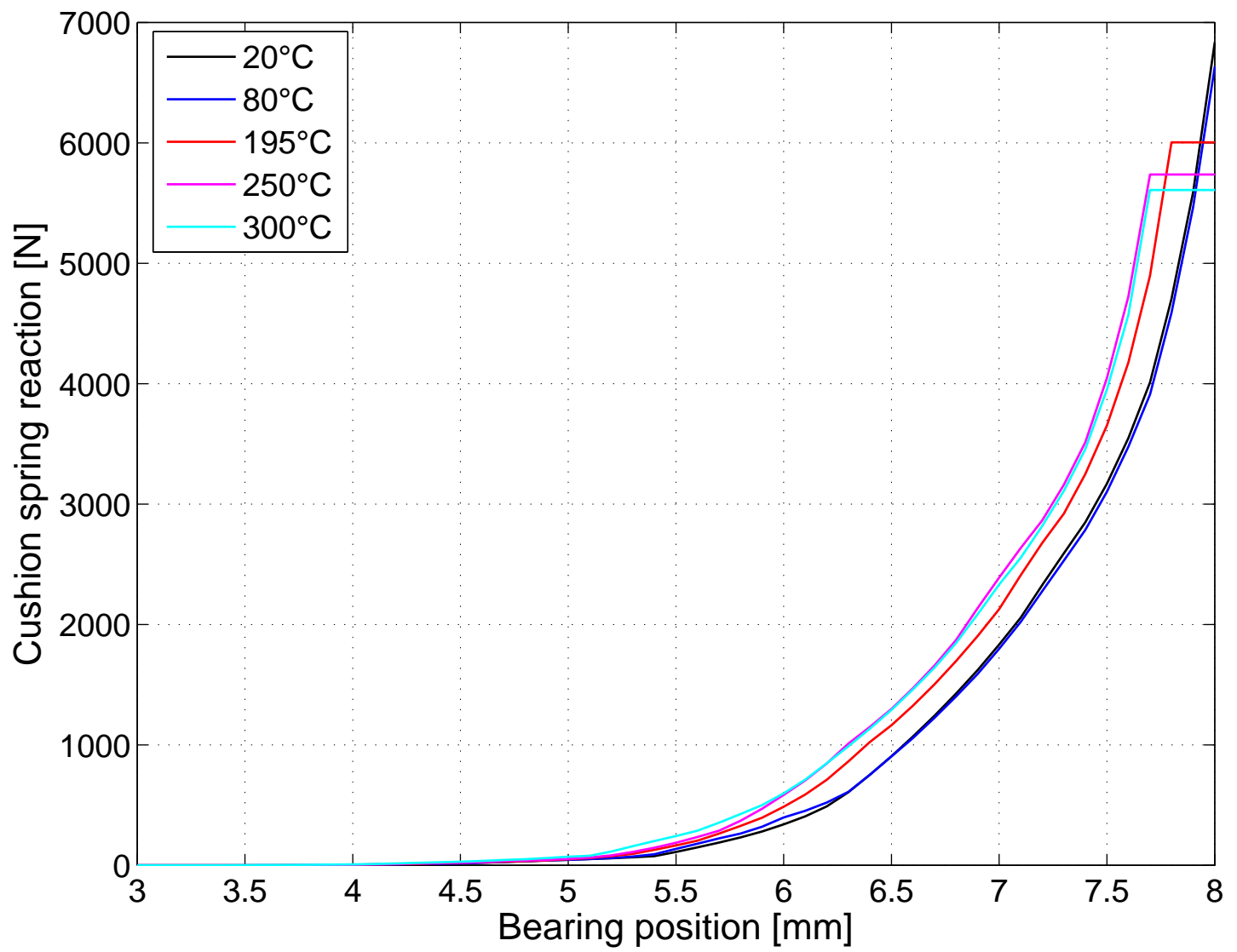


Fig. 5

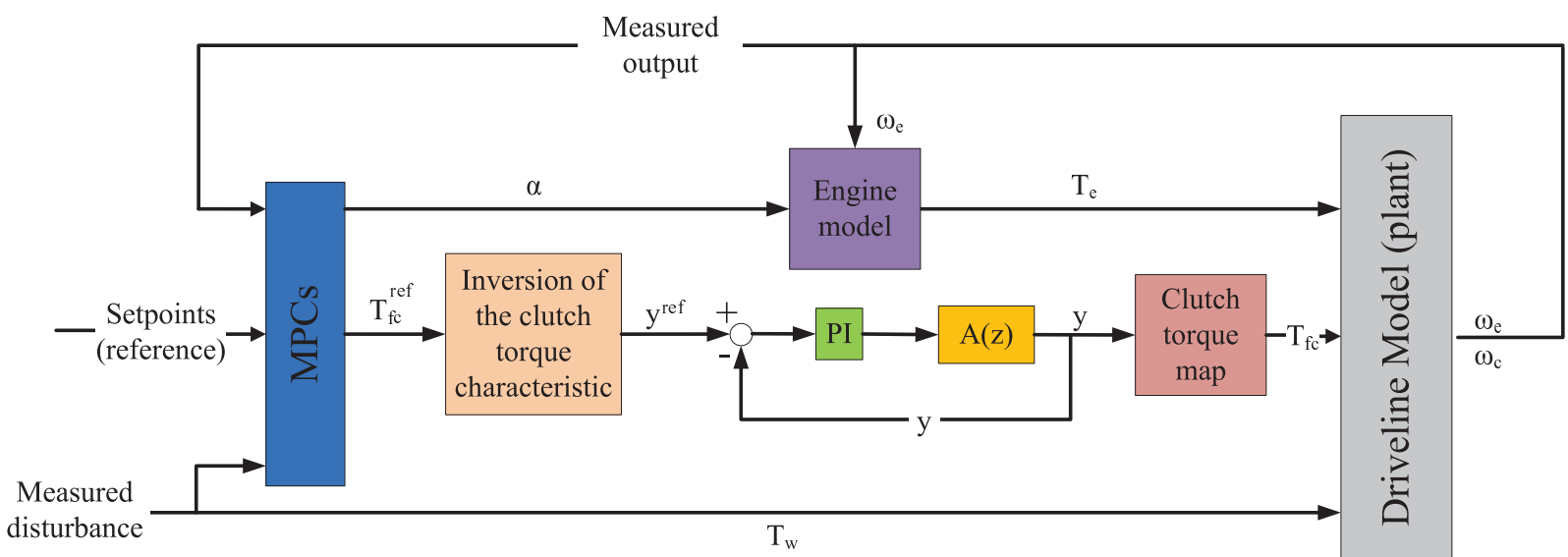


Fig. 6

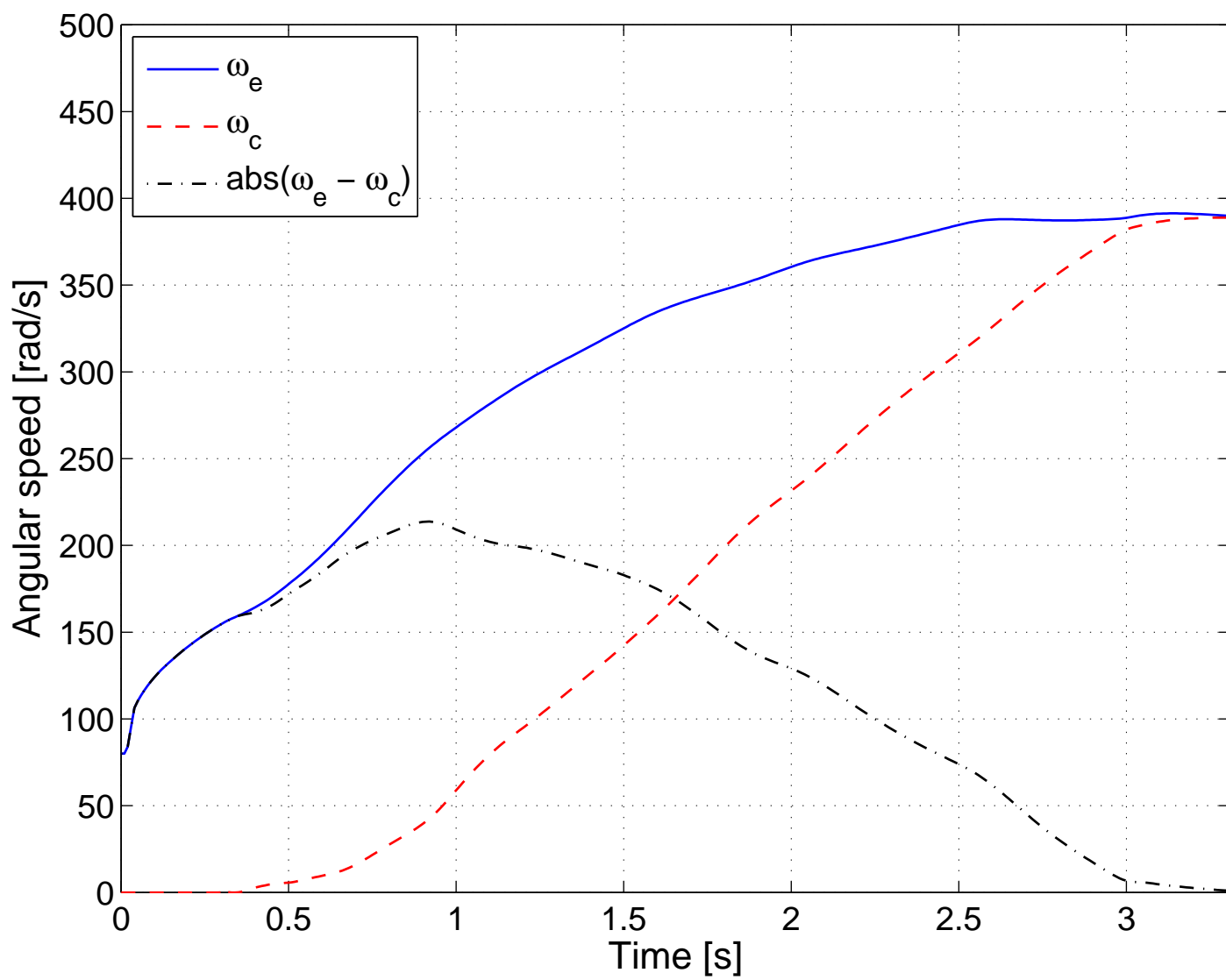


Fig. 7

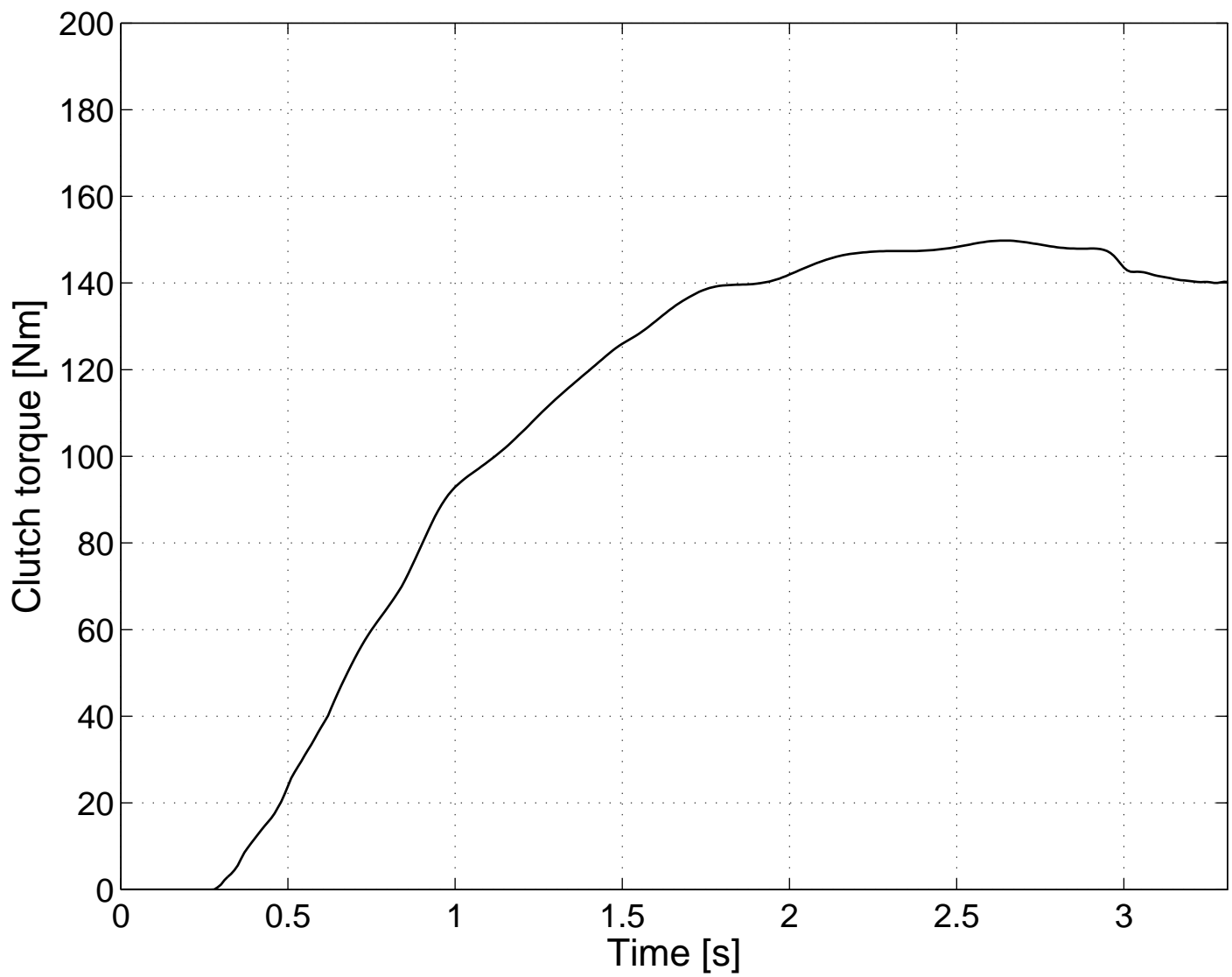


Fig. 8

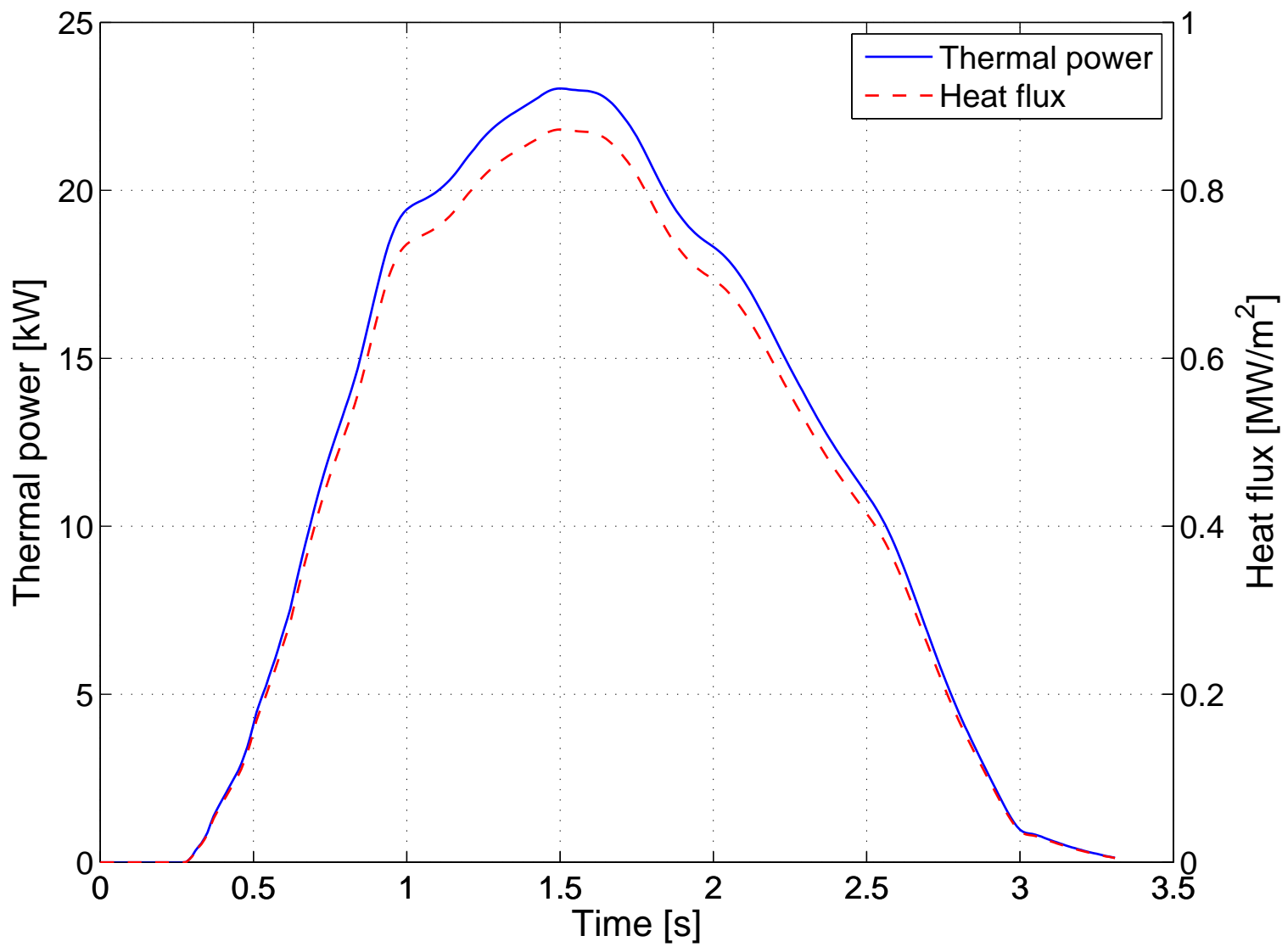


Fig. 9

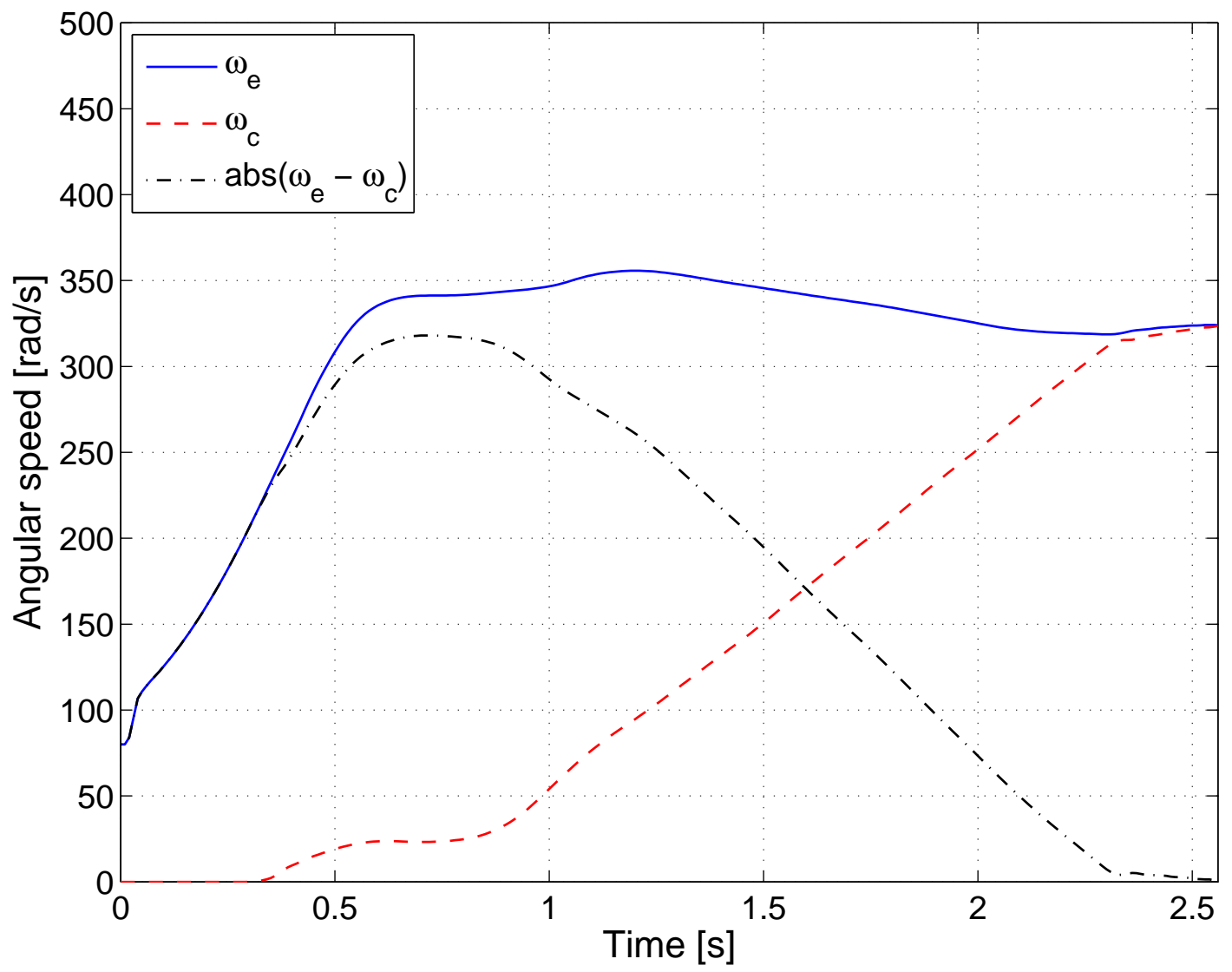


Fig. 10

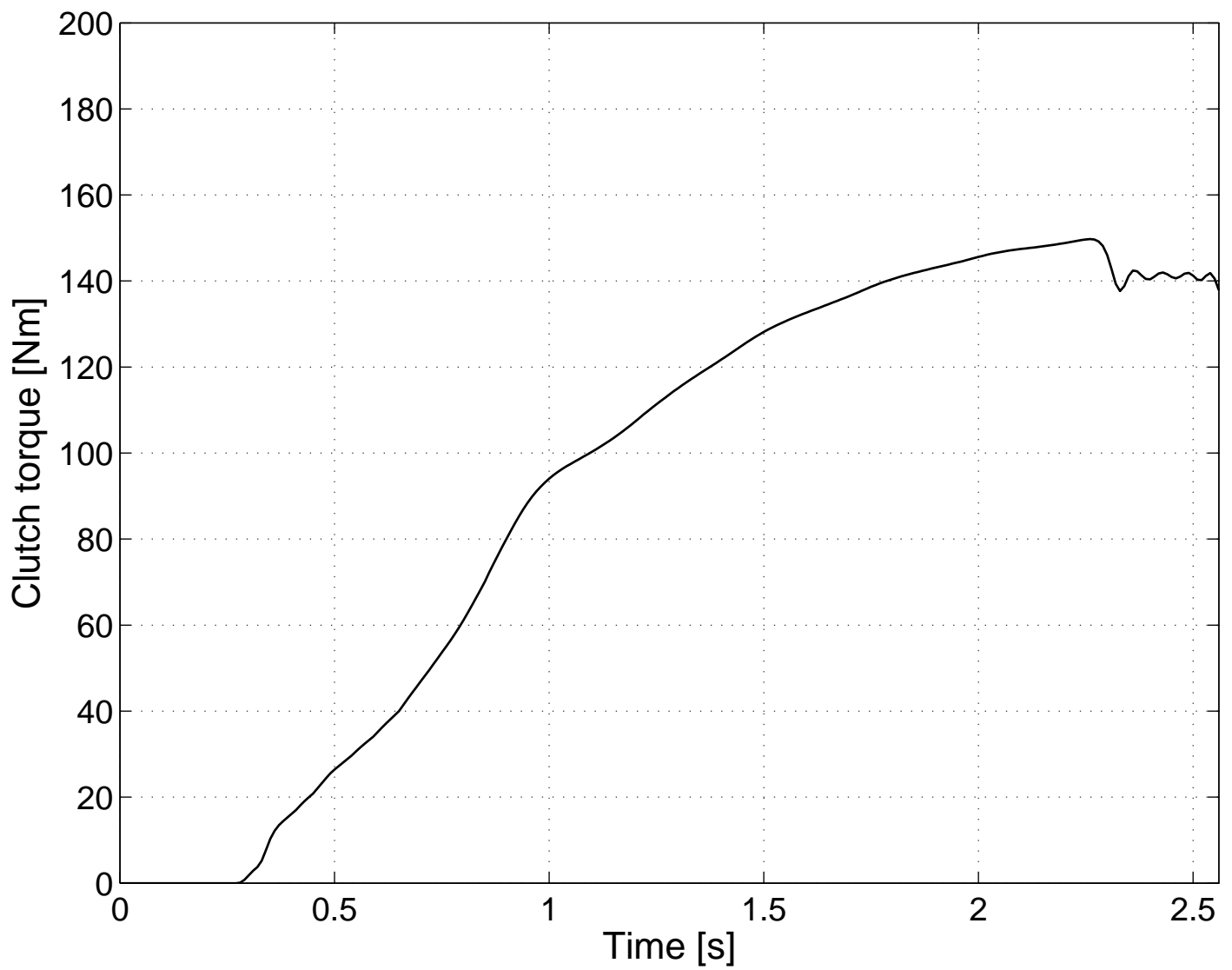


Fig. 11

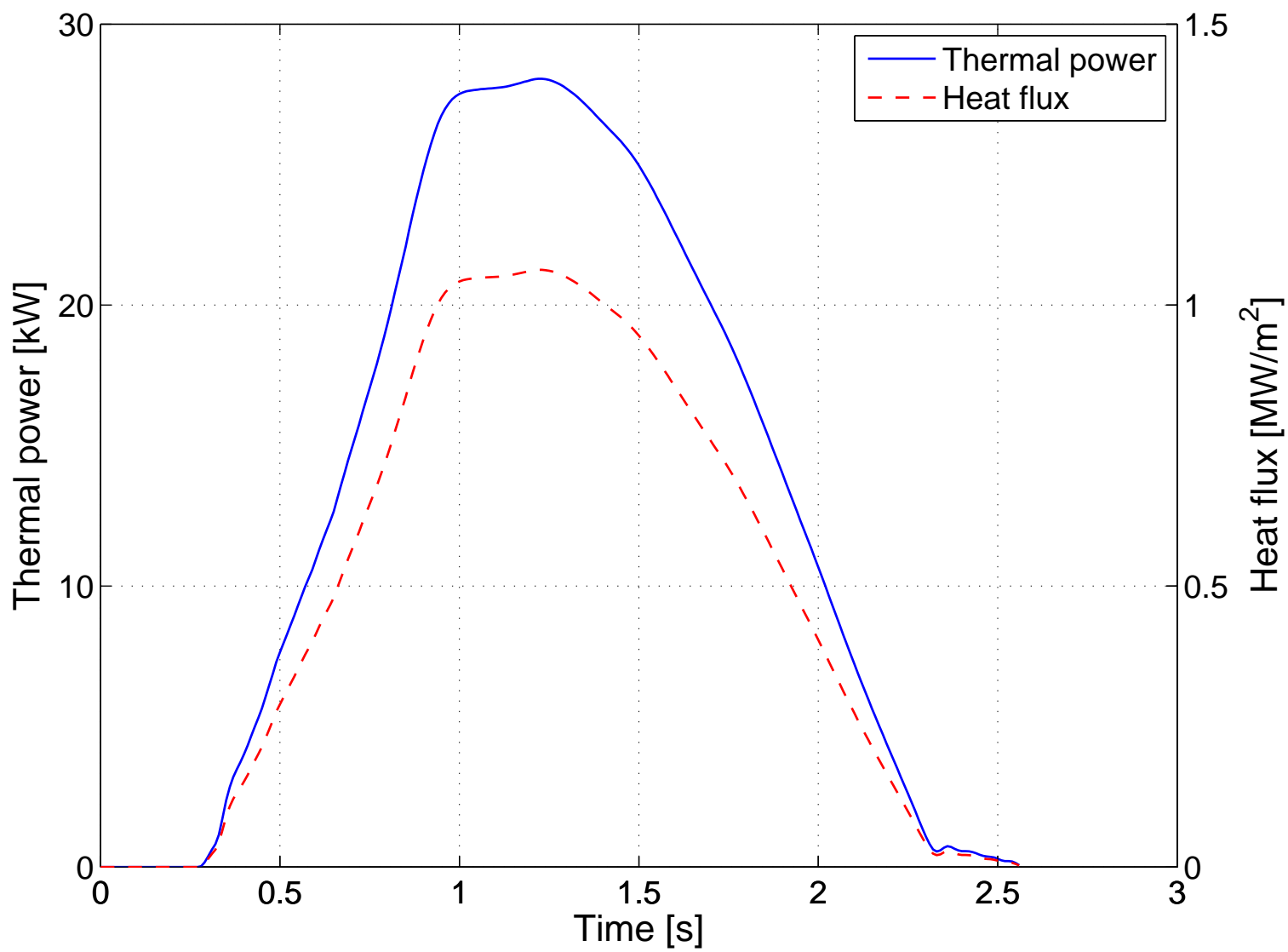


Fig. 12

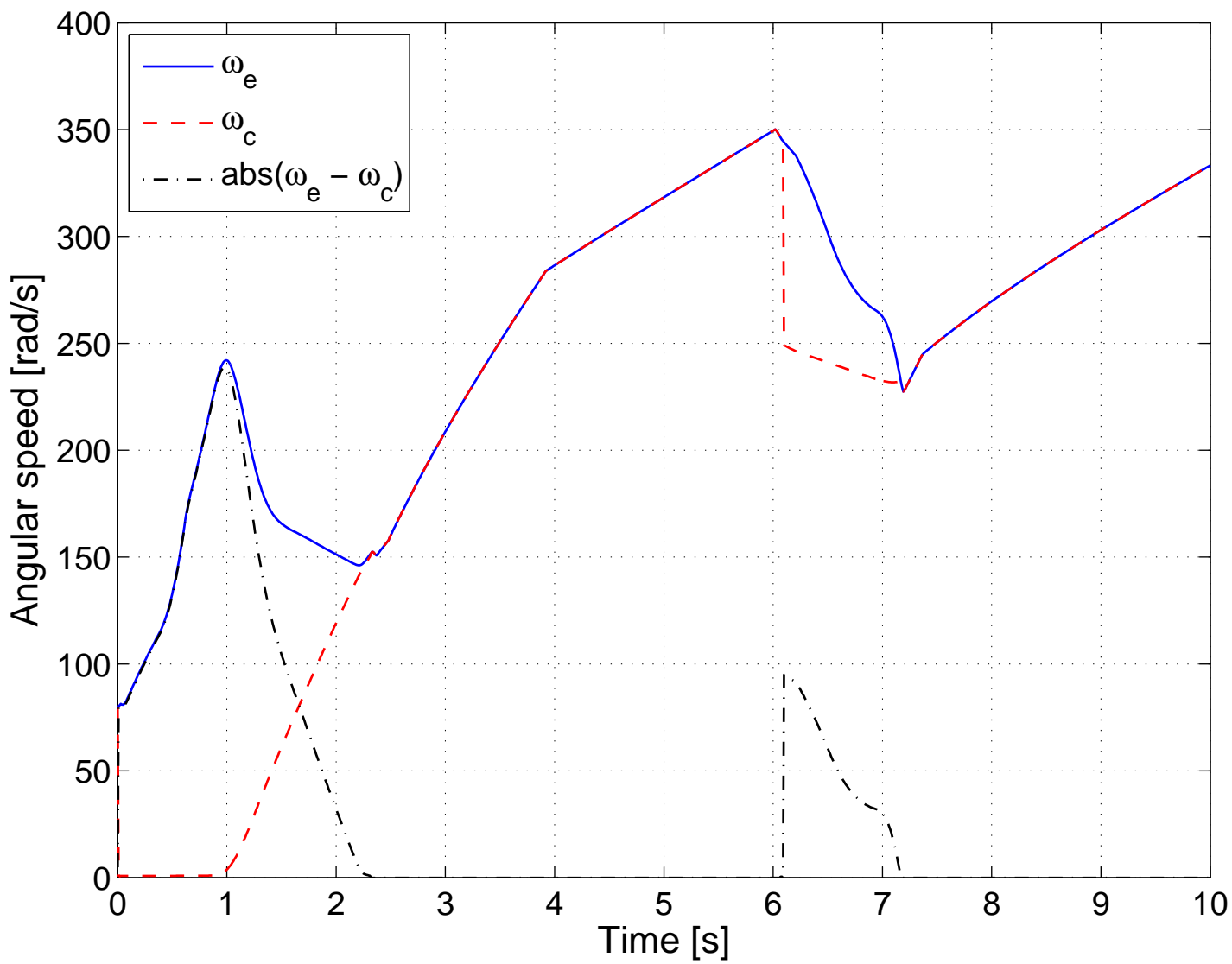


Fig. 13

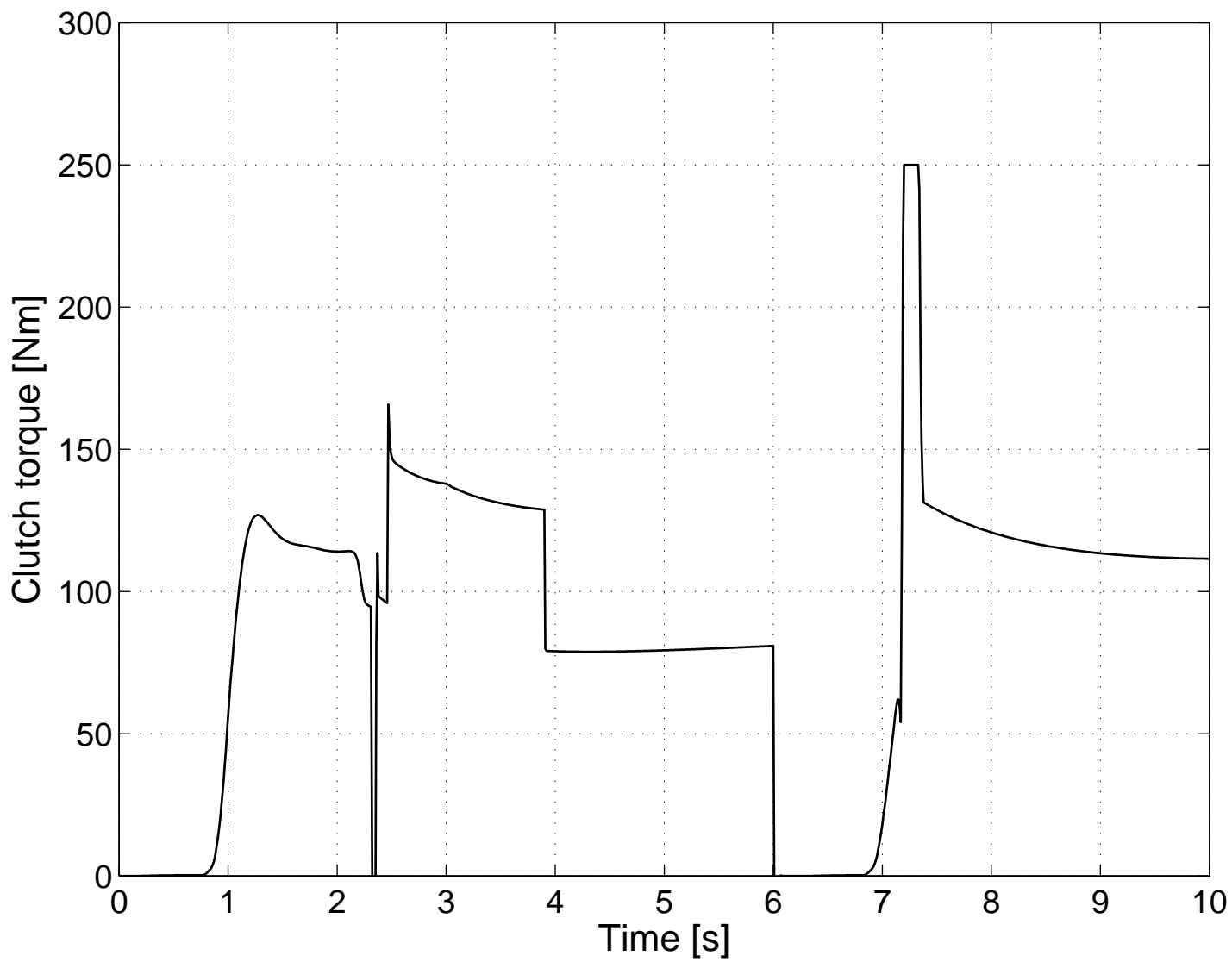


Fig. 14

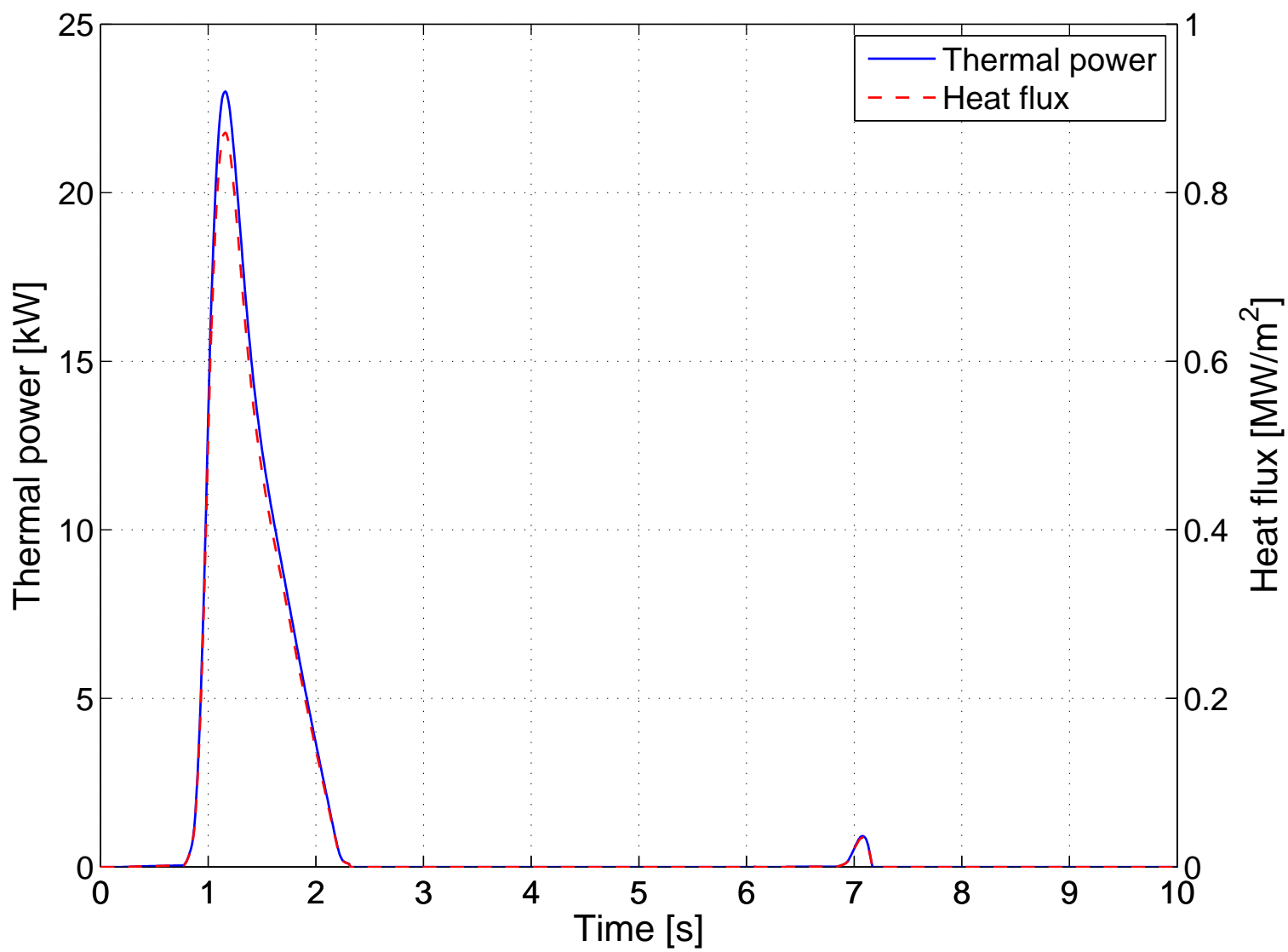
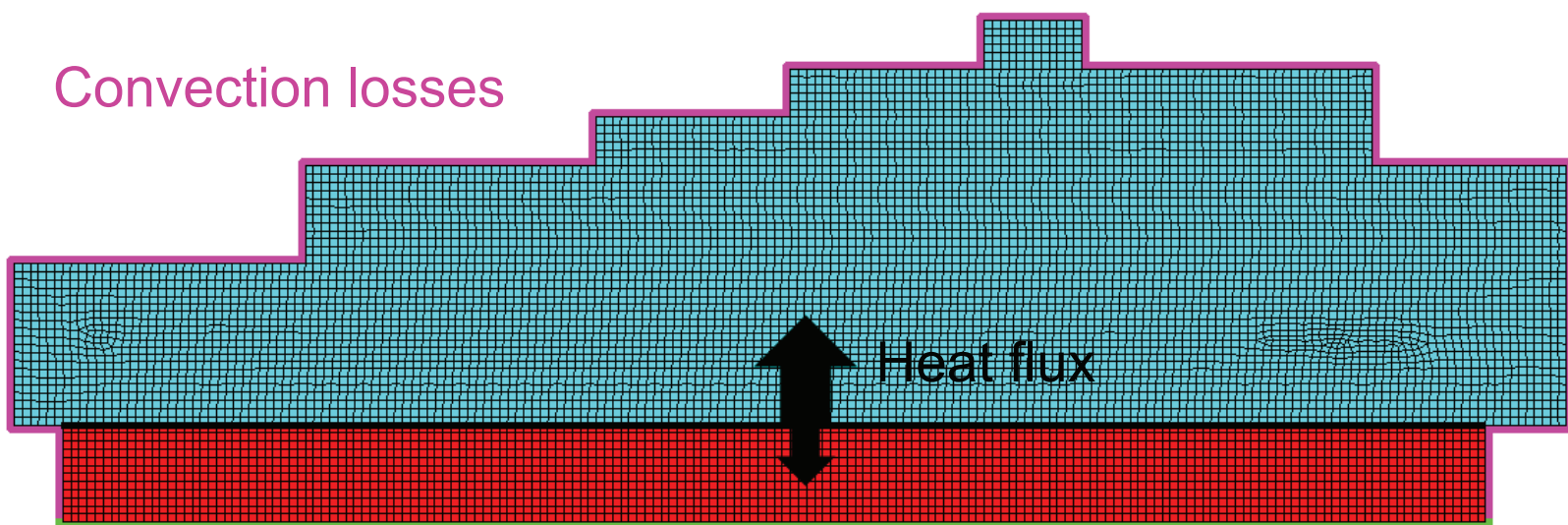


Fig. 15



Convection losses

Heat flux

Thermal symmetry condiction: adiabatic surface

Fig. 16

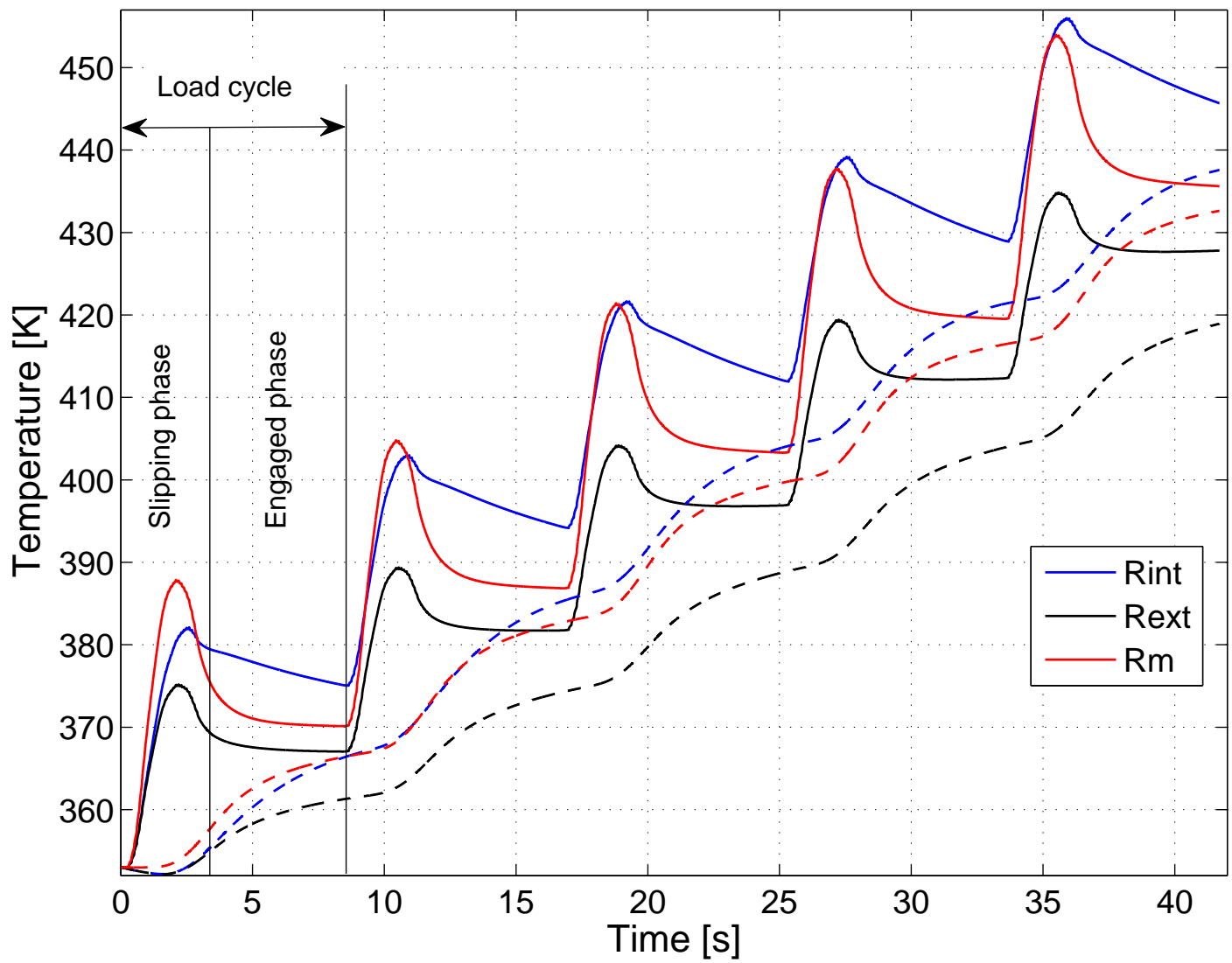


Fig. 17

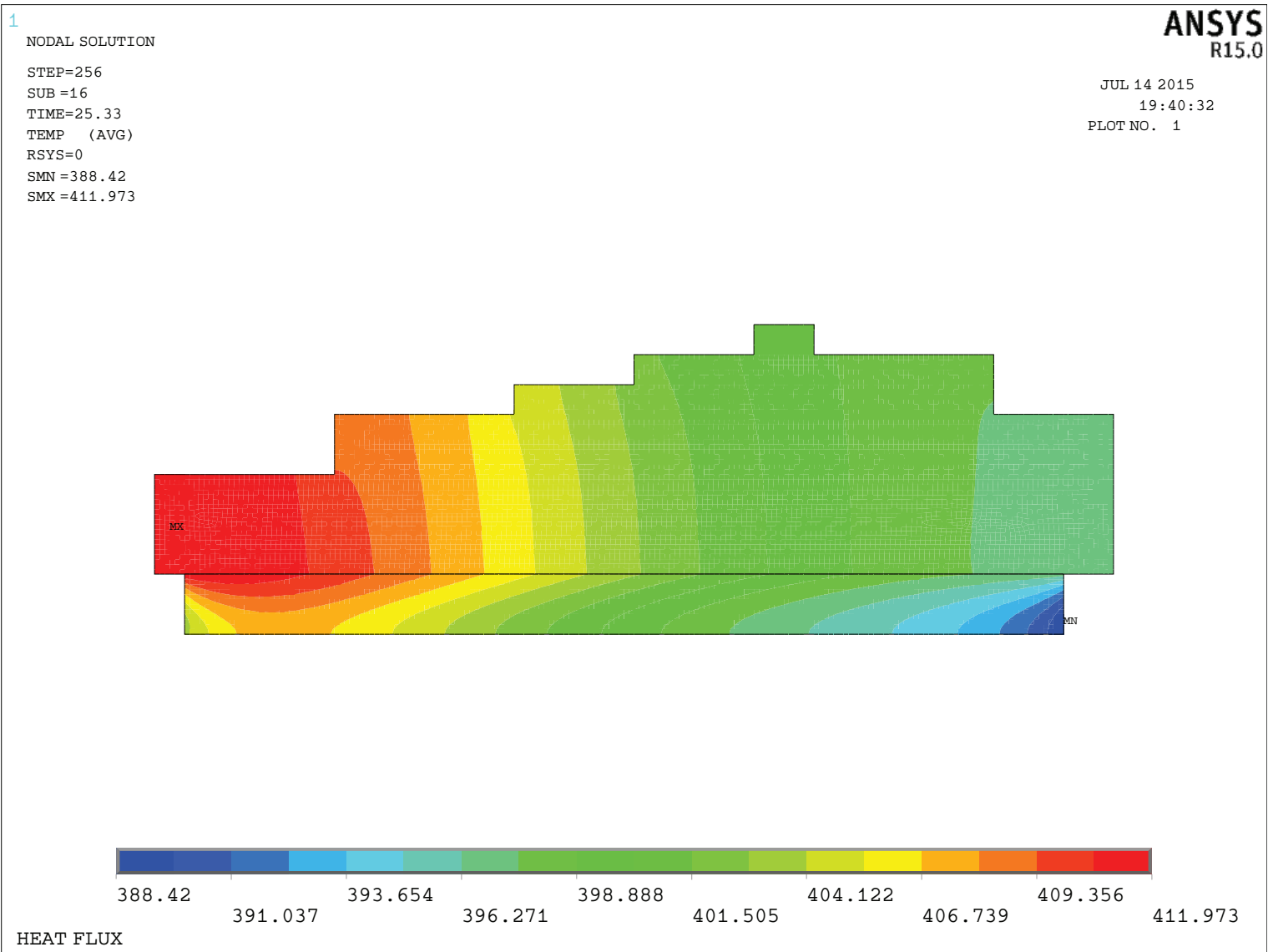


Fig. 18

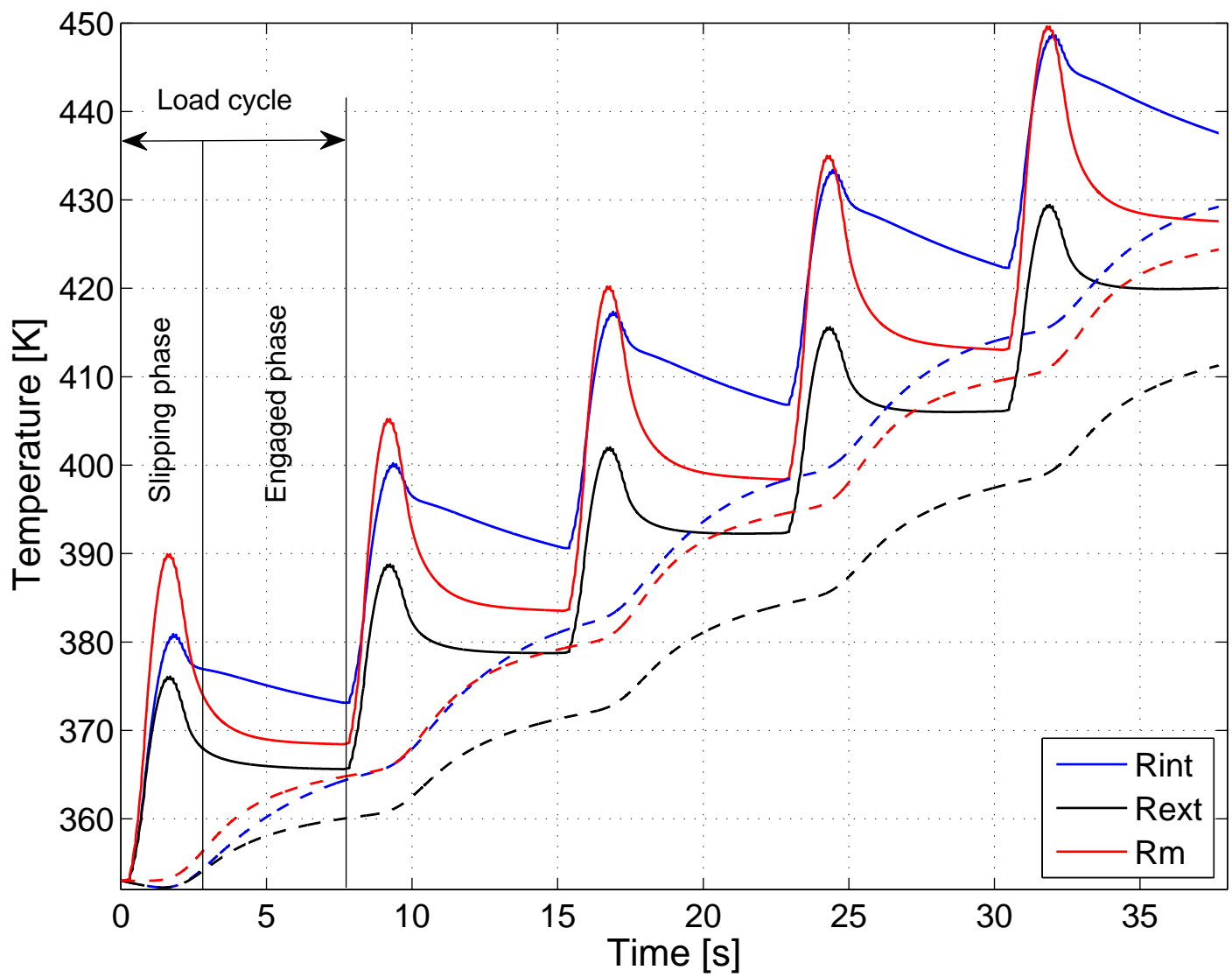


Fig. 19

